A dinosaur hunter who races the bulldozers *p. 1224*

Taking your best step forward *pp. 1230 & 1280*

Not enough neuroscience in addiction policies *p. 1237*

Science

$15
23 JUNE 2017
sciencemag.org

AAAS

THE SHAPING OF EGGS

Form reflects the needs of flight *pp. 1234 & 1249*

components that are required to assemble chromosomes in a test tube (*9*). Three components were found to be essential: histones, together with assembly factors that they require to load onto DNA; condensin; and topoisomerase II. The latter is an enzyme that allows DNA strands to pass each other, thereby preventing DNA from getting hopelessly tangled up.

How do histones contribute to chromosome assembly? Histones are abundant in the egg extract, and even if it were possible to remove them all, half of the histone octamers are already present in the *Xenopus* sperm chromatin. To study the role of histones in chromosome assembly, Shintomi *et al.* took advantage of the almost complete absence of histones from mouse sperm chromatin—in contrast to their abundance in *Xenopus* egg extract. The authors confirmed that mouse chromatin is converted into chromosomes in a *Xenopus* egg extract. Indeed, this occurred equally efficiently as with *Xenopus* chromatin. Instead of depleting histones, the authors depleted the essential histone chaperone Asf1 (anti-silencing function 1) from the egg extract, which is required for new histone deposition on DNA. Strikingly, chromosomes that were virtually free of histones efficiently assembled in the extract. At first sight, their appearance seemed hardly compromised by the absence of histones. This calls into question the textbook model of histones as the building block of chromosomes. Rather, it appears that condensin sets up much of the chromosome architecture, independently of histones (see the figure).

"...condensin sets up much of the chromosome architecture, independently of histones..."

On closer inspection, Shintomi *et al.* noted that these virtually histone-free chromosomes were somewhat wider than their usual counterparts, and their periphery appeared diffuse. In addition, they were susceptible to DNA unwinding or damage. Thus, although histones do not shape the chromosome, they contribute to DNA compaction and protection. Wrapping and thereby sequestering DNA is surely part of how histones compact and protect DNA. Another characteristic of a nucleosome is that it bends DNA. DNA enters and exits the nucleosome at an angle of approximately 70° (*3*). This produces a kink in the path of what is otherwise a rather stiff DNA molecule. The consequently rugged path of a nucleosome chain aids its compaction. It could also be that the very small amount of histones that are present on mouse sperm chromatin and that make it onto these "almost nucleosome-free" chromosomes make an important contribution by occasionally inflecting the path of the DNA.

The DNA kinking property of histones might also explain a little twist to the story. Vertebrate condensin comes in two types, condensin I and condensin II. Condensin II is present in low abundance in *Xenopus* egg extracts, and its depletion is usually hardly noticeable on the resultant chromosomes. However, in the absence of histones, condensin II becomes crucial for chromosome formation. The ability of either histones to bend DNA or of condensin II to stabilize a bent DNA conformation might be required as a basis for the action of the condensin I complex.

An important open question highlighted by the study of Shintomi *et al.* is how condensin shapes chromosomes. Condensin is a member of the structural maintenance of chromosomes (SMC) family of proteinaceous rings that topologically entrap DNA (*1*). They are thought to entrap not only one DNA, but to establish interactions between more than one DNA. How condensin selects two DNA strands to tether and the mechanism of tethering are not yet understood. It has been proposed that condensin stabilizes stochastic DNA contacts that arise from Brownian motion. Alternatively or additionally, condensin might actively move along DNA to extrude or expand DNA loops that are formed by the interaction between two DNAs (*10–12*). Genome-wide intrachromosomal DNA interaction maps are being made available by the DNA sequencing revolution (*13*). These inform our ideas of what exactly condensin has to achieve. The challenge is on to find biochemical and biophysical assays and new imaging techniques to explore the molecular mechanism of how condensin achieves the marvelous task of building these iconic chromosome structures. ■

REFERENCES

1. F. Uhlmann, *Nat. Rev. Mol. Cell Biol.* **17**, 399 (2016).
2. K. Shintomi, F. Inoue, H. Watanabe, M. Ohsugi, T. Hirano, *Science* **356**, 1284 (2017).
3. K. Luger, A. W. Mäder, R. K. Richmond, D. F. Sargent, T. J. Richmond, *Nature* **389**, 251 (1997).
4. M. Eltsov, K. M. MacLellan, K. Maeshima, A. S. Frangakis, J. Dubochet, *Proc. Natl. Acad. Sci. U.S.A.* **105**, 19732 (2008).
5. Y. Nishino *et al.*, *EMBO J.* **31**, 1644 (2012).
6. T. Hirano, T. J. Mitchison, *Cell* **79**, 449 (1994).
7. N. Saitoh, I. G. Goldberg, E. R. Wood, W. C. Earnshaw, *J. Cell Biol.* **127**, 303 (1994).
8. T. Hirano, R. Kobayashi, M. Hirano, *Cell* **89**, 511 (1997).
9. K. Shintomi, T. S. Takahashi, T. Hirano, *Nat. Cell Biol.* **17**, 1014 (2015).
10. T. M. K. Cheng *et al.*, *eLife* **4**, e05565 (2015).
11. G. Fudenberg *et al.*, *Cell Rep.* **15**, 2038 (2016).
12. T. Terekawa *et al.*, *BioRxiv* 137711 [Preprint]. 13 May 2017.
13. N. Naumova *et al.*, *Science* **342**, 948 (2013).

10.1126/science.aan8090

EVOLUTION

The most perfect thing, explained

The requirements of flight best explain the evolution of different egg shapes

By **Claire N. Spottiswoode**[1,2]

Every bird egg serves the same function: to protect and nourish the offspring within while it grows from two cells to a fully formed chick. Yet this identical function is served by a striking diversity of egg shapes. Explanations for both the origin and function of this diversity have remained little more than anecdotal (*1*). On page 1249 of this issue, Stoddard *et al.* (*2*) marry biophysics and ecology to provide a general theory that explains how and why diverse egg shapes arose. Based on a mathematical model, the authors predict that simple changes in the forces experienced by the shell membrane as the egg develops in the female's oviduct are sufficient to generate the observed egg-shape diversity across all birds. The selection pressure that best explains its evolution comes from the characteristic we most associate with birds: flight.

The authors began by mapping the diversity of egg shapes in nature. They measured the eggs of 1400 bird species in the Museum of Vertebrate Zoology at Berkeley, California, and plotted them in a space defined by two axes, starting at the origin with a perfect sphere (see the figure). Along one axis, an egg becomes more elongate, like a zeppelin (ellipticity); along the other, it becomes pointy at one end, like a raindrop (asymmetry). These two traits are sufficient to describe the bewildering variety of egg shapes seen in nature, but this diversity has clear limits. Some trait combinations do not exist. For example, eggs are never short but pointy, like a hot-air balloon (that is, with low ellipticity and high asymmetry; the empty space at the bottom right of the figure). The authors' next steps help to explain these limits to diversification.

Put an egg in a jar of vinegar for a couple of days until the shell has dissolved, wash

[1]*Percy FitzPatrick Institute of African Ornithology, DST-NRF Centre of Excellence, University of Cape Town, Rondebosch 7701, South Africa.* [2]*Department of Zoology, University of Cambridge, Downing Street, Cambridge CB2 3EJ, UK. Email: cns26@cam.ac.uk*

The two dimensions of egg shape

Two traits are sufficient to describe egg shapes found in nature (orange dots): ellipticity (elongation) and asymmetry (pointiness at one end). But egg diversity also has clear limits, as some trait combinations do not exist. Learn more about egg shape in an interactive graphic at http://vis.sciencemag.org/eggs.

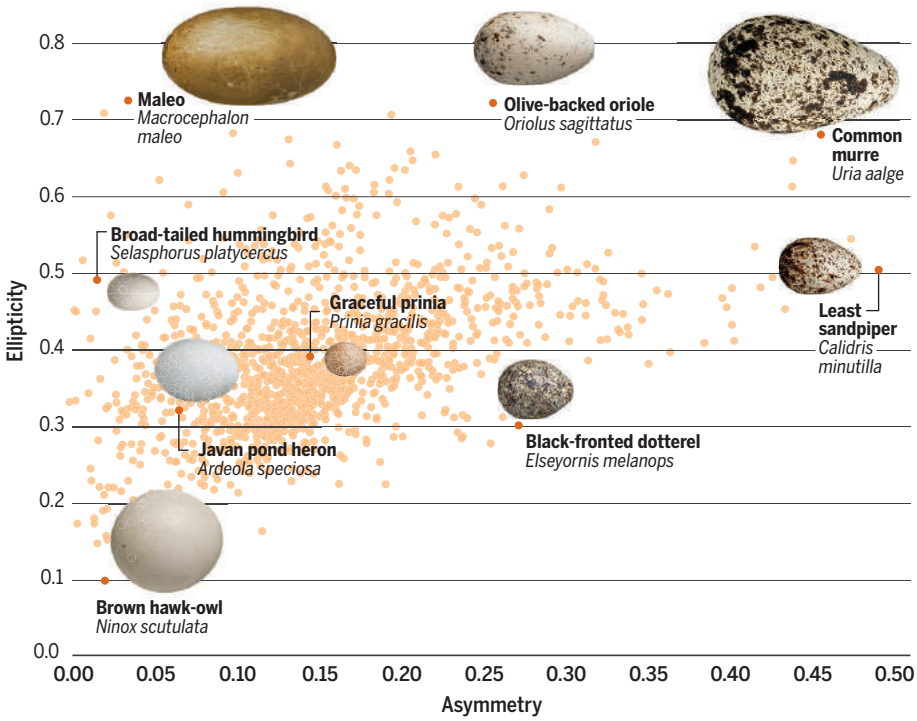

away the scum of calcium salts, and the wobbly remnant will be unmistakably egg-shaped (try this at home—it works) (*1*). It is this observation—that egg shape is dictated by the membrane over which the shell is laid down, rather than the shell itself—that inspired the authors to develop a biophysical model for how variation in egg shape is generated.

Their model shows that the diversity observed in nature can be generated by iteratively varying two parameters: first, the resistance of the membrane to pressure along the egg's long axis versus pressure around its girth, which varies across the egg according to gradients in membrane thickness and fiber type, orientation, and density; and second, the pressure difference across the membrane that arises as the egg inflates, grows, and squeezes against the oviduct walls. Egg shapes not seen in nature would require improbably rapid changes in membrane properties over a short distance. The avocado-like shapes of freakish common murre eggs coveted by egg collectors a century ago (*1*) suggest that extreme forms can arise in species that normally produce eggs with more usual shapes (see the figure). Had these odd-shaped eggs been fertile (we don't know), would natural selection ever have favored them?

In the final part of their study, Stoddard *et al.* investigate such adaptive questions. Open any ornithological textbook and you will find intriguing but ultimately parochial hypotheses to explain why different egg shapes have evolved: pointy eggs don't roll off cliffs; different shapes fit best together in different-sized clutches; birds that eat more calcium can afford more shell (*3*, *4*). Stoddard *et al.* test systematically whether any of these hypotheses hold up at a large scale, by mapping egg shape across a phylogenetic tree and testing for consistent associations with ecology. They find that traditionally invoked ecological explanations such as nest type and clutch size are not consistently associated with particular egg shapes at a broad taxonomic scale.

Instead they find consistent support for a simple hypothesis (*5*). Birds are streamlined for flight. Perhaps streamlined birds need narrower eggs to negotiate their narrower pelvis, and because the only way to fit a chick into a narrower egg is to make the egg longer, elliptical or asymmetric eggs result. This hypothesis predicts that species under strong selection for flight-related adaptations—such as migrants and aerial insectivores—should have elliptical or asymmetric rather than spherical eggs. The authors use an index of aerodynamic wing shape as a proxy for such selection, and find that this is by far the best predictor of egg shape. Swifts that live almost all of their lives on the wing have elliptical eggs. Sandpipers that traverse the globe have elliptical, asymmetric eggs. Puffbirds and trogons of tropical forests that may rarely leave their territories tend to have relatively spherical eggs. So, too, do flightless ostriches, but not penguins—perhaps because they must be streamlined to "fly" underwater. Within specific taxonomic groups, additional correlations suggest that other demands, such as clutch size, do further modulate egg shape, but none applies generally across all birds. Why, then, are there no hot-air balloon–shaped eggs? Not only do they appear developmentally hard to produce, but perhaps they offer no obvious selective advantage over a spherical egg: They are still inconveniently wide, with little increase in volume.

Stoddard *et al.* conclude that variation in egg shape at a broad scale is best explained by variation in the need to fly. But although satisfyingly general, this discovery will be far from the final word. A bird's egg was famously described by abolitionist Thomas Wentworth Higginson as "the most perfect thing in the universe" (*6*), but this apparent perfection is most likely the sum of multiple ecological, structural, and developmental compromises. It remains unclear why egg shapes tend toward being spherical in the absence of strong selection for powered flight. Do asymmetry and ellipticity carry costs, such as making an egg easier to break into or harder to break out of? And why has natural selection solved the streamlining problem with elongate and symmetric eggs in some species, and elongate and asymmetric eggs in others—that is, what best explains the variation along the x axis of the figure? Did elongate eggs repeatedly evolve in concert with narrower pelvises, and do their shell membranes vary in thickness and composition in the way that Stoddard *et al.*'s model predicts? Their paper opens up a rich seam for researchers to explore.

Stoddard *et al.*'s study was made possible by a museum collection of 49,175 eggs that obsessive fieldmen (for they were always men) found in their concealed nests, blew out, and labeled, and that committed museum staff curated upon their collectors' deaths. Egg collecting is now deeply unfashionable and rightly illegal. But from its heyday in the late 19th to the mid-20th century, it has bequeathed to us data that can yield wonderful evolutionary insights, as Stoddard *et al.*'s study underlines. We should continue to treasure the institutions that protect them. ■

REFERENCES

1. T. R. Birkhead, *The Most Perfect Thing: Inside (and Outside) a Bird's Egg* (Bloomsbury, 2016).
2. M. C. Stoddard *et al.*, *Science* **356**, 1249 (2017).
3. I. J. Lovette, J. W. Fitzpatrick, Eds., *Handbook of Bird Biology* (Wiley-Blackwell, ed. 3, 2016).
4. F. B. Gill, *Ornithology* (Freeman, ed. 3, 2007).
5. J. B. Iverson, M. A. Ewert, in *Egg Incubation: Its Effect on Embryonic Development in Birds and Reptiles*, D. C. Deeming, M. W. J. Ferguson, Eds. (Cambridge Univ. Press, 1991), pp. 101–116.
6. T. W. Higginson, *Atl. Mon.* **10**, 368 (1862).

10.1126/science.aan2517

RESEARCH ARTICLE

EVOLUTION

Avian egg shape: Form, function, and evolution

Mary Caswell Stoddard,[1]* Ee Hou Yong,[2] Derya Akkaynak,[3,4] Catherine Sheard,[5] Joseph A. Tobias,[6]† L. Mahadevan[7]*†

Avian egg shape is generally explained as an adaptation to life history, yet we currently lack a global synthesis of how egg-shape differences arise and evolve. Here, we apply morphometric, mechanistic, and macroevolutionary analyses to the egg shapes of 1400 bird species. We characterize egg-shape diversity in terms of two biologically relevant variables, asymmetry and ellipticity, allowing us to quantify the observed morphologies in a two-dimensional morphospace. We then propose a simple mechanical model that explains the observed egg-shape diversity based on geometric and material properties of the egg membrane. Finally, using phylogenetic models, we show that egg shape correlates with flight ability on broad taxonomic scales, suggesting that adaptations for flight may have been critical drivers of egg-shape variation in birds.

About 360 million years ago, the ancestors of all terrestrial vertebrates began to colonize habitats out of the water. This transition was facilitated by a critical evolutionary innovation: the development of the amniotic egg, complete with a specialized set of membranes and a shell (*1*). Among the most familiar of these structures are the calcified eggs of birds, which exhibit a variety of sizes and shapes (*2*): spherical in owls, elliptical in hummingbirds, conical in shorebirds, and a range of forms in between. However, we still know surprisingly little about the function of egg shape or the physical mechanism by which shape variation arises (*1*, *3*).

Hypotheses proposed for the adaptive function of egg shape typically invoke a decrease in egg loss for cliff-nesting birds laying conical eggs that roll in a tight circle (*4*); an increase in incubation efficiency when egg shape is associated with the number of eggs in a clutch (*5*, *6*); or other advantages related to strength, diet, and development. For example, spherical eggs might be advantageous because the sphere is uniformly strong and would be robust to incidental damage in the nest. Spherical eggs, with their minimal surface-area-to-volume ratio, also require the least amount of shell material for a given volume (*7*) and possibly optimize gas exchange by providing a large surface area for pores (*8*). In contrast, conical eggs may be beneficial because they can accommodate an increased concentration of pores at the blunt end, creating a specialized respiratory site for accelerated neural development in precocial birds (*8*). Moreover, conical eggs may protect the blunt end (from which chicks usually hatch) from debris contamination or, in colonial breeders, increase resistance to impacts because a larger proportion of the eggshell is in contact with the substrate (*9*). Finally, it has also been proposed that adaptations for flight influence egg shape indirectly through the morphology of the pelvis, abdomen, or oviduct (*10*). Previous studies investigating the diversity of egg shape have been hampered by small sample size, reflecting the lack of comprehensive data on egg morphometry and life history traits, and therefore most of the above hypotheses

[1]Department of Ecology and Evolutionary Biology, Princeton University, Princeton, NJ 08544, USA. [2]Division of Physics and Applied Physics, School of Physical and Mathematical Sciences, Nanyang Technological University, Singapore 637371, Singapore. [3]Leon S. Charney School of Marine Sciences, Department of Marine Technologies, University of Haifa, Israel. [4]Interuniversity Institute of Marine Sciences, Eilat, Israel. [5]Department of Archaeology and Anthropology, University of Bristol, 43 Woodland Road, Bristol BS8 1UU, UK. [6]Department of Life Sciences, Imperial College London, Silwood Park, Buckhurst Road, Ascot SL5 7PY, UK. [7]Departments of Organismic and Evolutionary Biology, and Physics, and Paulson School of Engineering and Applied Sciences, Kavli Institute for Bionano Science and Technology, Wyss Institute for Biologically Inspired Engineering, Harvard University, Cambridge, MA 02138, USA.
***Corresponding author. Email: mstoddard@princeton.edu (M.C.S.); lmahadev@g.harvard.edu (L.M.)** †These authors contributed equally to this work.

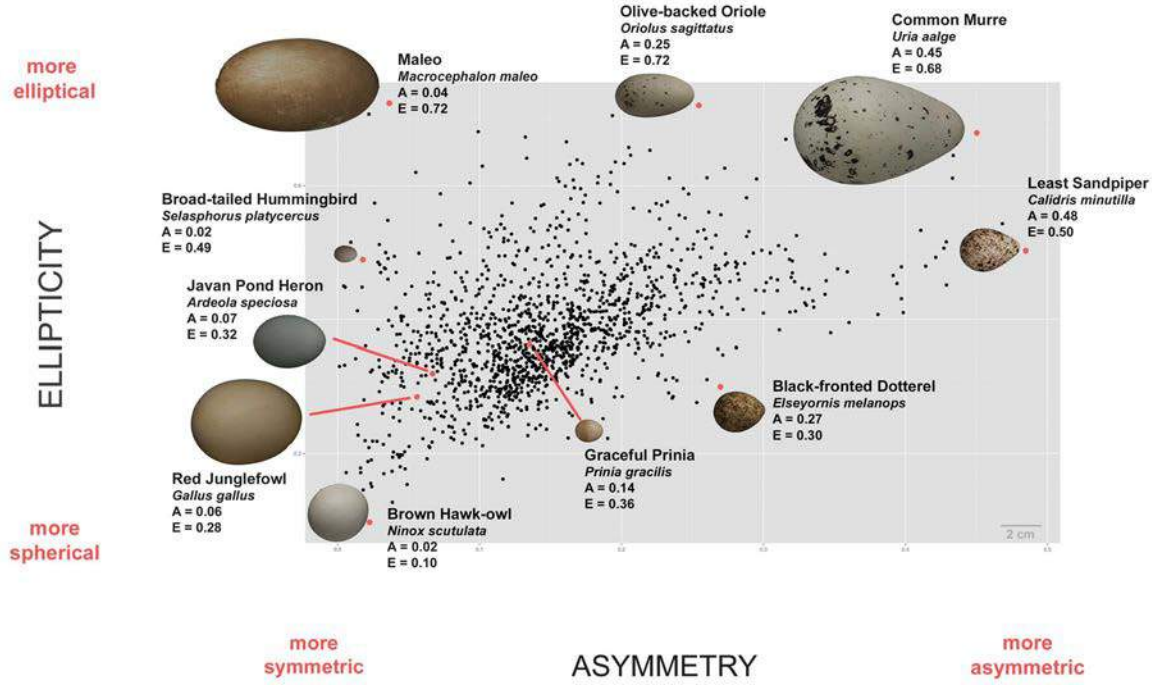

Fig. 1. Morphospace of avian egg shape. Average egg shapes for each of 1400 species (black dots), illustrating variation in asymmetry and ellipticity, as defined in the text. Images of representative eggs are shown alongside their associated points in morphospace (colored red) to highlight variation in shape parameters. [Egg images (shown on the same relative scale) are copyright of the Museum of Vertebrate Zoology, Berkeley. Image details and sources are given in Data S2.]

remain untested, particularly within a phylogenetic framework (*3*).

Here, we resolve these issues by quantifying egg shape using a morphometric analysis of 49,175 eggs representing ~1400 (~14% total) species in 35 extant orders, plus two extinct orders (Data S1). We then use these data to (i) quantify the observed morphologies in a two-dimensional (2D) morphospace for egg shape; (ii) provide a mechanistic model of how the egg is shaped in the oviduct; and (iii) test major hypotheses about egg-shape variation in the context of key life history and environmental variables on a global scale. As a first step, we plotted egg shape in a 2D morphospace that characterizes the asymmetry A and ellipticity E of axisymmetric eggs (Fig. 1 and figs. S1 and S2), in line with earlier proposals that egg shape should be quantified using plane projective geometry (*11*, *12*). This approach showed that the occupied morphospace is triangular (Fig. 1 and fig. S3), with the bounding vertices corresponding to eggs that are symmetric and spherical, symmetric and elliptical, and asymmetric and elliptical. Interestingly, the occupied morphospace lacks spheroidal, asymmetric eggs, somewhat similar in shape to a hot air balloon (fig. S3), a point to which we will return. A preliminary investigation of morphospace data highlights two key observations.

First, egg shape is a continuum, with no divisions between traditionally defined shape classes. Egg shapes range from A = 0.001 (*Streptopelia bitorquata*, island collared dove) to 0.485 (*Calidris minutilla*, least sandpiper) and E = 0.097 (*Ninox scutulata*, brown hawk-owl) to 0.724 (*Macrocephalon maleo*, maleo) (Fig. 1). A density map (fig. S4) shows that many species converge on egg shapes with $A \in [0.1, 0.2]$ and $E \in [0.3, 0.4]$, similar in shape to the egg of the graceful prinia (*Prinia gracilis*) but not to the familiar "egg shape" of the chicken ancestor, the red junglefowl (*Gallus gallus*) (Fig. 1). The most densely occupied region of morphospace includes eggs laid by 26 species in 16 families and three orders (fig. S4). The traditional egg-shape classes often presented in the literature fail to identify this canonical egg form, with no single egg-shape class falling near the true most common egg shape (fig. S5).

Second, avian clades differ widely in their distribution across egg morphospace (Fig. 2 and fig. S6), although substantial within-clade variation generates overlaps between clades (Fig. 2). Clades also differ in the extent of within-clade variation, as quantified by the area of the minimum convex hull containing species within each avian order (Fig. 2, fig. S7, and table S1). For example, Charadriiformes (shorebirds) (n = 154) occupy a far greater area than do Passeriformes (perching birds, including songbirds) (n = 740) (Fig. 2 and table S1) (*13*), despite the fact that Passeriformes are more speciose than Charadriiformes by more than an order of magnitude. Furthermore, bird eggs span a morphospace that differs from that occupied by theropod dinosaurs, nonavian reptiles, and monotreme mammals, particularly in terms of asymmetry (fig. S8). Elongate, asymmetric eggs evolved before the ancestor of extant birds: Some theropod dinosaurs laid asymmetric eggs (*14*, *15*), and a survey of Cenozoic fossil bird eggs shows that considerable variation in egg shape arose before extant birds (*16*). However, extant birds colonized some new regions of morphospace unoccupied by any other extinct or extant group of vertebrates, including regions of very high (>0.45) asymmetry and very low (<0.2) ellipticity (fig. S8).

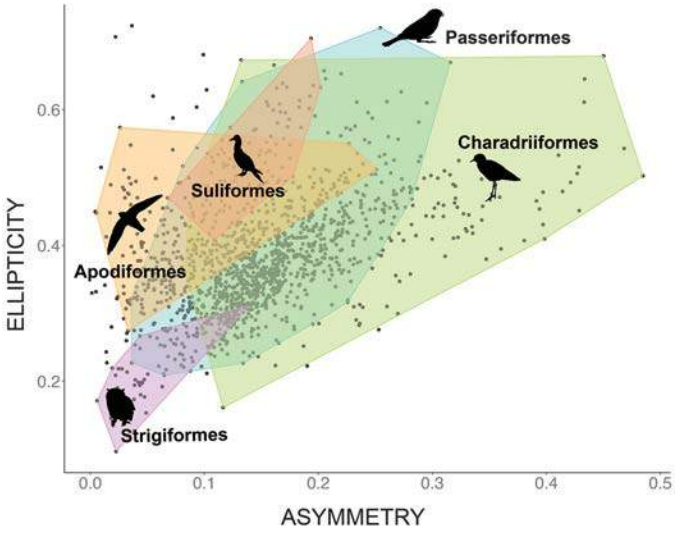

Fig. 2. Partitioning of egg variation among avian orders. Black dots (one per species) (n = 1400) show the morphospace of egg shape in two dimensions (asymmetry and ellipticity). Colored polygons show the minimum convex hull plotted for all species within a subset of avian orders (Strigiformes, Apodiformes, Suliformes, Passeriformes, and Charadriiformes). Overlap in egg shape is extensive, even among ecologically and phenotypically dissimilar orders. However, some orders (e.g., Charadriiformes) occupy a much larger region of egg morphospace than others. For silhouette details, see Fig. 4.

A biophysical model of egg shape

These patterns reveal how egg shape varies across birds and pave the way to a mechanistic theory that can predict shape. Such a theory can generate predictions about physical processes in the oviduct that may facilitate or constrain (fig. S3) the evolution of egg-shape variation. In developing this theory, we assume that egg shape is fixed by the shell membranes rather than by the shell itself, evidence for which comes from x-ray imaging (*17*) and experiments showing that an egg retains its shape even after shell removal (*3*). Egg shape is likely established as the egg moves through the isthmus (*8*), one of the final portions of the oviduct.

In the isthmus, the egg is surrounded by its membrane (actually a double membrane), a meshwork of collagenous fibers (*18*). A recent study in chickens suggests that the magnum-isthmus junction, where membrane deposition is initiated, is the site of shape determination; before reaching this part of the oviduct, eggs are more spherical and less asymmetric (*19*). After leaving the isthmus, the egg enters the shell gland, where the biomineralized calcium carbonate shell is deposited.

Building on these insights, a biomechanical approach based on pressure differences across a closed elastic membrane of varying thickness is a natural starting point (*20*–*22*). Our proposed model makes the simplest assumption consistent with a nonspherical shape for a pressurized closed elastic membrane: that the membrane properties are inhomogeneous owing to variations in thickness and material properties. When such a membrane is pressurized, it distends and takes up a form determined by two types of variation across the egg's surface: (i) variation in applied pressure difference across the surface; and (ii) variation in the membrane's thickness and material properties across the surface. We extend previous work that has alluded to these ideas qualitatively (*20*–*22*) by constructing a mathematical model that connects to the available experimental literature and emphasizes the central role played by the membrane. This model accounts for (i) differential forcing on the membrane from external muscular forces and internal pressure and (ii) variations in membrane properties in the axial and azimuthal directions.

We assume that egg growth and morphogenesis proceed as follows: (i) the enclosed membrane is deposited around the sphere of yolk and albumen; (ii) internal pressure is created inside the membrane-enclosed sac, which could arise from fluid being actively pumped into the sac (i.e., water absorption or "plumping"), differential elasticity of the isthmus wall, muscular contractions, or some combination of these; and (iii) the variation in membrane material properties (including collagen fiber composition/direction, elastic modulus, and thickness) contributes to differential distortion in response to pressure in the axial and azimuthal directions. Ellipticity results from the fact that the membrane is easier to stretch along the oviduct axis (pole to pole) than perpendicular to it (around the egg's girth). Asymmetry, however, requires a difference in membrane material properties between the two poles. In all cases, the egg is axisymmetric, meaning that variation in shape, pressure, and/or membrane properties is symmetric across the egg's major (longitudinal) axis.

The shape of an axisymmetric egg can be completely described by a planar curve C, with radial and angular coordinates $[r(\sigma), \theta(\sigma)]$ as a function of a curvilinear material coordinate σ (Fig. 3). As the membrane distends under pressure, we define the axial extension ratio $\lambda_s = \partial s/\partial\sigma$, where s is the stretched coordinate, and the azimuthal

extension ratio $\lambda_\varphi = r/r_0$, with the associated principal strains $e_{ss} = (\lambda_s^2 - 1)/2; e_{\varphi\varphi} = (\lambda_\varphi^2 - 1)/2$. Assuming a simple linear constitutive relation linking stress and strain (*23*, *24*), we may then write the thickness-integrated axial and azimuthal stresses (Fig. 3) as $t_s = Ae_{ss} + Be_{\varphi\varphi}; t_\varphi = Ae_{\varphi\varphi} + Be_{ss}$, where $A(\sigma)$, $B(\sigma)$ are the thickness-integrated axial and azimuthal stretching stiffnesses of the egg membrane, respectively, and depend on the local elastic moduli as well as the thickness of the membrane. This allows us to write the equations of mechanical equilibrium for the egg membrane in the normal and tangential directions as $P = \kappa_s t_s + \kappa_\varphi t_\varphi, \partial(rt_s)/\partial s - t_\varphi \partial r/\partial s = 0$, in terms of the principal curvatures of the membrane $\kappa_s = \frac{\partial\theta}{\partial s}$; $\kappa_\varphi = \sin\theta/r$, and the constant pressure difference across the membrane P. Here, we have ignored the free boundaries associated with the fact that the egg is not in contact with the walls of the oviduct near the poles, because we assume that the shape is preserved even in the absence of the walls. There will be a small correction to the shape if we account for the effects of finite membrane bending stiffness and the free boundaries. Making the variables in the above equations dimensionless (*13*) allows us to rewrite them in terms of the ratio of the azimuthal to the axial stiffness $\mu(\sigma) = B(\sigma)/A(\sigma)$ and the scaled effective pressure $p(\sigma) = P/A(\sigma)$ (*24*). The solutions of these equations for prescribed forms of these functions give us the shape of the egg; indeed, the spatial variation of $\mu(\sigma)$, $p(\sigma)$ (as a function of location across the egg's surface) controls both the asymmetry and ellipticity of the egg (*13*).

To constrain these two functions, we note that early work (*25*) suggests that there is considerable variation in the properties of chicken eggshell membrane along its longitudinal axis, including variation in membrane thickness $h(\sigma)$, membrane density, membrane nitrogen, and membrane packing index. This indicates that density of packing

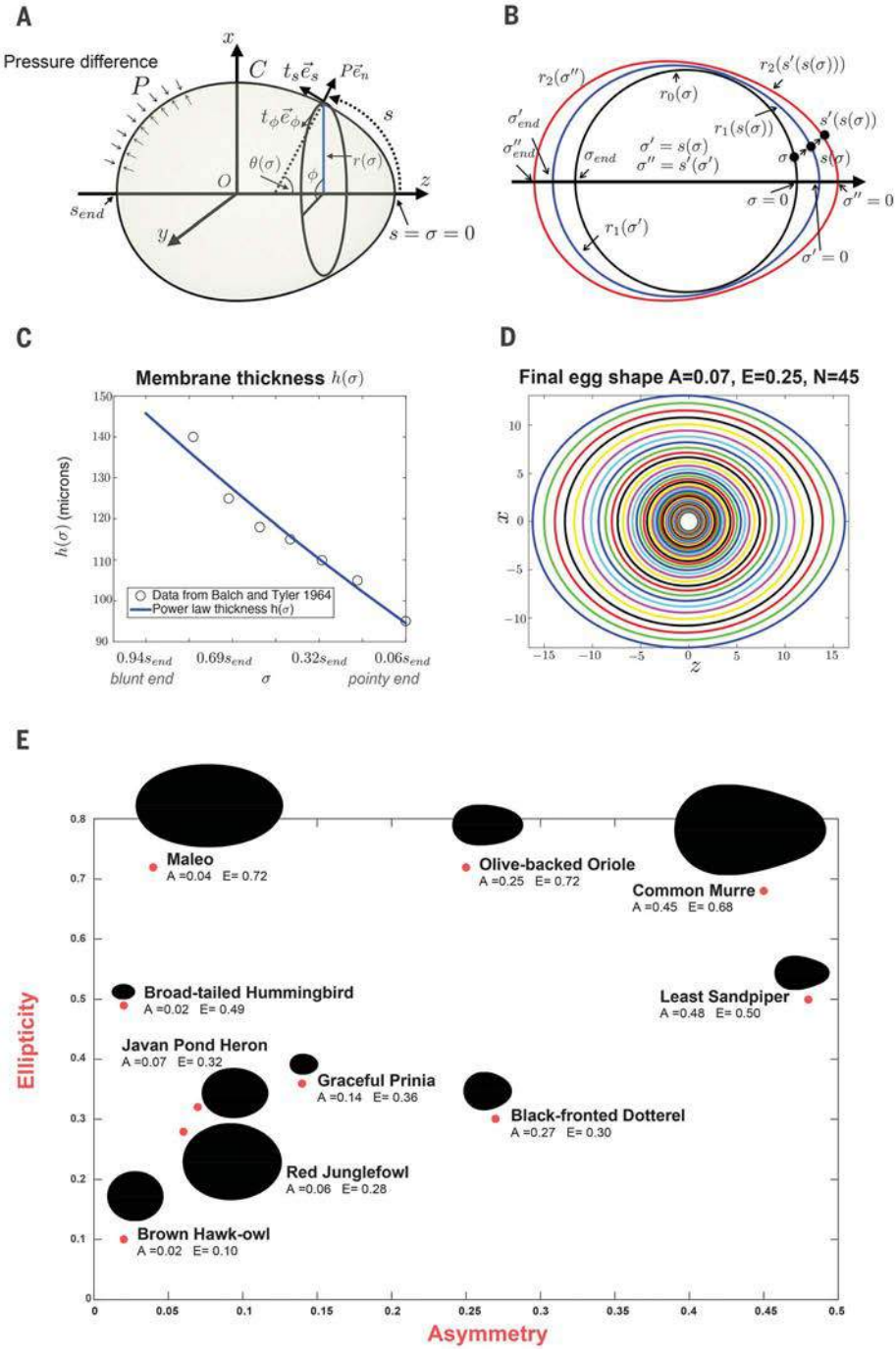

Fig. 3. Biophysical model of egg shape. (**A**) An axisymmetric egg is described by a planar curve C that, when revolved around the axis of symmetry (z axis), yields the surface of the egg, with radial and angular coordinates $[r(\sigma), \theta(\sigma)]$ parametrized by a curvilinear material coordinate σ defined relative to one of the poles of the egg. There is a uniform pressure difference P across the membrane, a thickness-integrated axial stress $t_s(\sigma)$ and a thickness-integrated azimuthal stress $t_\phi(\sigma)$ that together characterize the three principal stresses at every location along the axisymmetric egg membrane. Here, e_n is the unit vector in the normal direction and e_s and e_ϕ are the two orthogonal tangent directions pointing in the axial and azimuthal directions along the membrane surface. The stiffnesses in the axial and azimuthal direction are given by $A(\sigma)$, $B(\sigma)$ and link the stresses to the elastic strains driven by the pressure difference across the membrane (see text and supplementary materials for details). O is the Cartesian origin. (**B**) Schematic representation of the reparameterization/growth process. The initial reference shape $r_0(\sigma)$ grows to $r_1(\sigma)$ after one growth step, driven by the scaled pressure $p(\sigma)$ and the ratio of azimuthal to axial stiffness $\mu(\sigma)$ (see text and supplementary materials for details). This new shape is then used as a reference shape in the next growth step, yielding an iterative approach to morphogenesis. (**C**) Experimentally observed variations in egg membrane thickness taken from Fig. 3 of Balch and Tyler (*25*) allow us to fit a simple power law and parametrize the functions $A(\sigma), B(\sigma)$ (see supplementary materials) and therefore $p(\sigma)$, $\mu(\sigma)$. (**D**) A spherical egg grows into a classic chicken egg that is both elliptical and asymmetrical in 45 discrete growth steps following the protocol in (B). (**E**) The full avian morphospace can be generated using different functional forms for the scaled ratio of azimuthal to axial stiffness and the scaled pressure, $\mu(\sigma)$, $p(\sigma)$, respectively (see text and supplementary materials for details).

of the fibers in the membrane, and thus the membrane's elastic modulus, must vary from pole to pole due to variations in the type (e.g., collagen), orientation, density, and amount of material. Based on these observations, and on the membrane thickness data from (*25*), we use simple power-law functions for the scaled pressure, $p(\sigma)$, which depends on $A(\sigma)$. Starting with a spherical egg shape that corresponds to a constant thickness and elastic moduli of the egg membrane, we can generate nonspherical eggs by iteratively changing $p(\sigma)$ and $\mu(\sigma)$ away from a constant value. For example, by making the membrane slightly thicker at one pole, the scaled pressure will be larger at the opposite pole because $A(\sigma)$ will be smaller (thinner) there, so that the egg will become asymmetrical. This serves as a new initial shape on which we can make another incremental change in the membrane thickness, or equivalently in $A(\sigma)$, $B(\sigma)$, and solve the governing equations to get the new shape. In Fig. 3, B to D, we show how to derive the classic shape of a chicken egg as the number of growth steps N is varied (see also fig. S9). It is worth noting that our procedure yields egg shape but cannot predict absolute egg size because it uses rescaled variables. For example, if the pressure and membrane material properties are rescaled appropriately, this will result in larger eggs with the same shape.

Changing the functions $p(\sigma)$ and $\mu(\sigma)$ by varying the parameters in the power-law form allows us to generate egg shapes that span the full avian egg morphospace (Fig. 3E), as well as counterfactual egg shapes that do not appear in nature (fig. S10) (*13*). These counterfactual shapes are typically associated with strong and unusual variations in $\mu(\sigma)$, $p(\sigma)$ due to very localized variations in membrane thickness, mechanical properties, or both. Therefore, either the eggs of living birds are constrained (because the evolution of extreme variation in membrane properties is challenging) or such shapes have been strongly selected against (because the evolution of bizarre shapes is possible but maladaptive).

Testing functional hypotheses for egg-shape variation

Having quantified and mechanistically described egg shape, we investigated the evolution of diverse egg shapes by performing comparative analyses using recent phylogenetic hypotheses for the backbone (*26*) and tips (*27*) of the avian tree. Focusing on 1209 species in our data set for which molecular sequence data exist, we first assembled a phylogenetic tree onto which we mapped egg size (approximated by the length of the egg's major axis), asymmetry, and ellipticity (Fig. 4) (*13*). Egg size and shape vary markedly across this tree (Fig. 4), with increases in asymmetry and/or ellipticity occurring in parallel across different lineages—for example, highly asymmetric eggs evolved independently in penguins and in shorebirds.

To test functional explanations for the evolution of these diverse egg shapes, we compiled a data set with biometric, life history, and environmental parameters for all species in our sample. This included adult body mass, diet, clutch size, nest type, nest location, chick developmental mode (e.g., precocial), and environmental details (latitude, temperature, and average precipitation), calculated from geographical range polygons using standard techniques (*13*). We also used biometric measurements from museum specimens to calculate the hand-wing index (HWI), a standard proxy for flight efficiency and dispersal ability in birds (*13*, *28*, *29*). We computed HWI as the ratio of Kipp's distance (the distance between the tip of the longest primary and the tip of the first secondary feather) to total wing chord (distance between the carpal joint and wingtip) (*29*). Although HWI correlates with dispersal distance and migratory behavior in birds (*13*), we note that neither dispersal distance nor migration completely captures the essence of flight ability, because many bird species (e.g., some shorebirds and hummingbirds) fly well even though they are nonmigratory with low dispersal. Using HWI as an index of flight ability sidesteps this issue because even resident species with stronger and more frequent flight tend to have narrower and more pointed wingtips (high HWI), whereas species with weaker and less frequent flight tend to have shorter, more rounded wingtips (low HWI) (*13*). These assorted parameters allowed us to run Bayesian phylogenetic mixed-effect models to explore the extent to which various adaptive hypotheses predict avian egg shape on a global scale (tables S2 to S5) (*13*).

According to these analyses, egg length is predicted by adult body mass, clutch size, diet, and developmental mode (table S2A). In most cases,

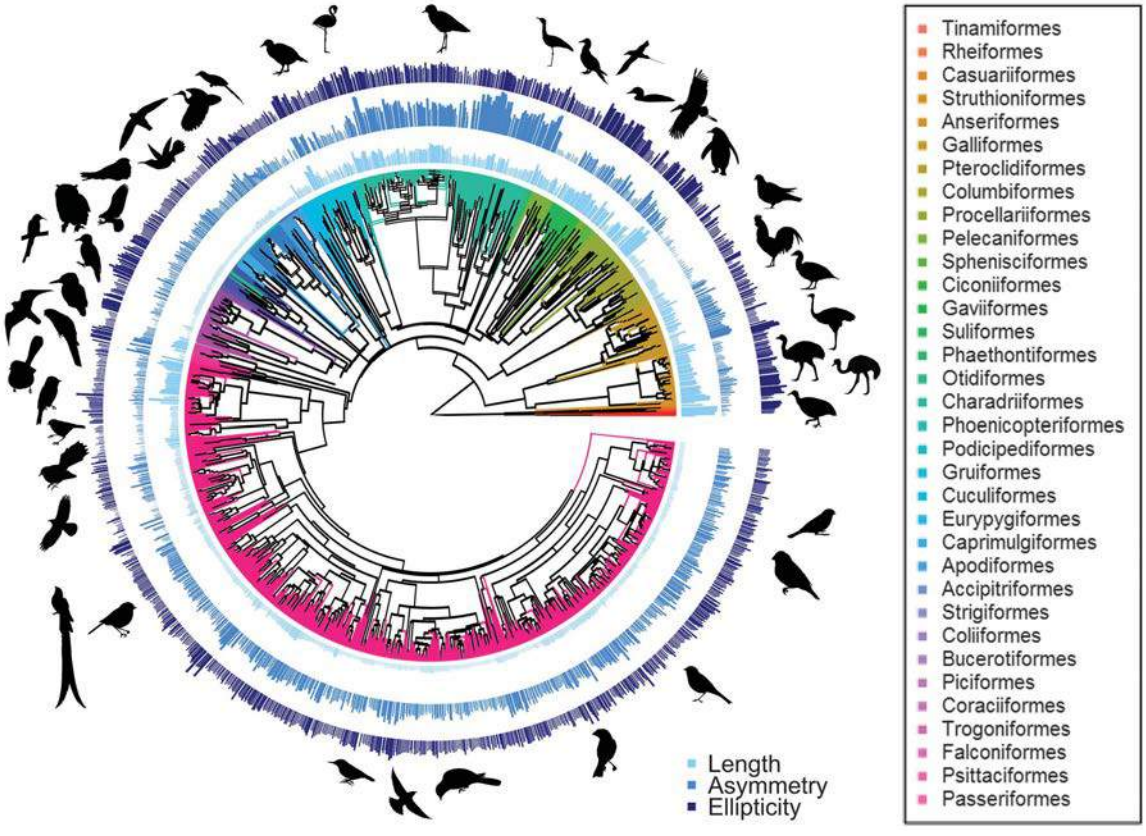

Fig. 4. Evolutionary patterns of egg-shape diversity. A phylogeny of 1209 species in our sample for which molecular sequence data exist, based on (*26*) and (*27*). For each species, the average egg length (light blue), asymmetry (medium blue), and ellipticity (dark blue) are represented by line lengths at branch tips. Silhouettes for representative species in each order are shown (details and image sources in Data S2).

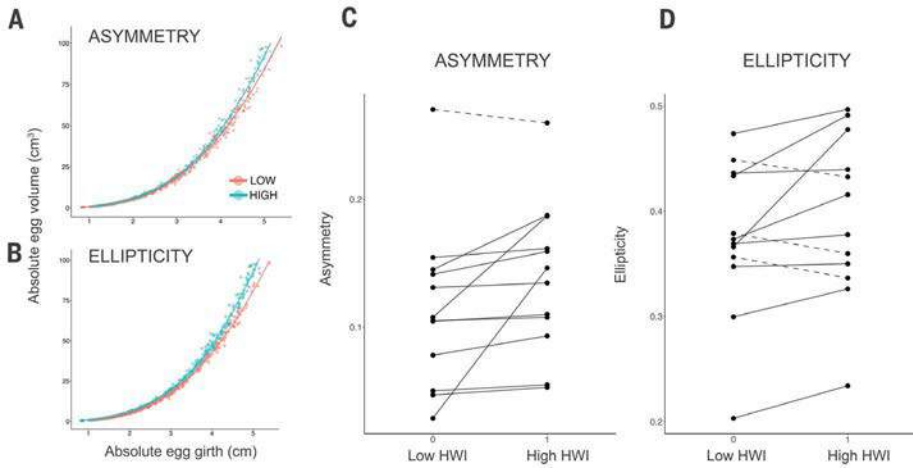

Fig. 5. Egg shape, egg volume, and flight ability. (**A** and **B**) For a given egg girth, birds increase egg volume by increasing asymmetry and/or ellipticity. In our data set, eggs that are more (A) asymmetric and (B) elliptical tend to have larger volumes for a given egg girth (width). Average egg girth (*x* axis) is calculated directly from images; egg volume (*y* axis) is derived from Baker (*11*). Eggs with high (upper 50% of all species) asymmetry (A) or ellipticity (B) are shown in turquoise; eggs with low (lower 50% of all species) asymmetry (A) or ellipticity (B) are shown in red. For clarity, we omitted eggs with the highest volumes (top 5% of species). (**C** and **D**) Comparison of egg asymmetry (C) and ellipticity (D) between species with high and low flight ability in the 12 most speciose orders in our sample. We divided extant species in each order according to HWI to directly compare between those with low HWI (lower 50%) and high HWI (upper 50%). Increased HWI (i.e., flight ability) is often associated with increased asymmetry or ellipticity (solid lines) and less often with decreased asymmetry or ellipticity (dashed lines).

these relationships support existing hypotheses, given that shorter eggs are associated with larger clutches and longer eggs are associated with a higher-calcium diet, larger adult body mass, and greater chick precociality. These findings suggest that egg size is regulated, at least in part, by life history characteristics and spatial constraints in the nest. In contrast, we found that egg shape (asymmetry and ellipticity) is not related to clutch size, developmental mode, environmental factors, or nest characteristics (table S2, B and C). These analyses consider variation across the entire avian clade, and on this taxonomic scale we find no support for the hypothesis that asymmetric eggs evolve more often in cliff-nesting birds or that egg shape is related to clutch size, which is consistent with our preliminary morphospace analysis (figs. S11 and S12). Although theoretically optimal egg shapes for different-sized clutches have been proposed in the context of incubation efficiency (*5*), these optima fall outside the true occupied morphospace of natural eggs for all but two clutch sizes ($n = 3$, $n = 9$) (fig. S11).

Instead, egg shape is correlated with egg size (captured by the first principal component PC1 of egg length and adult body mass) and HWI, with birds tending to lay eggs that are more asymmetric or more elliptical if they have a high HWI and/or if the eggs are larger (table S2, B and C). In addition, ellipticity is significantly predicted by the second principal component PC2 of egg length and body mass, such that birds with larger eggs than expected given their body mass lay more elliptical eggs (table S2C). Given that HWI is positively related to flight efficiency (*13*, *28*, *29*), these results raise the intriguing possibility that adaptations for flight may be key drivers of egg-shape variation in birds. This is consistent with a range of observations suggesting that key adaptations for high-powered flight—including reduced body size, a reduced abdominal cavity, and the loss of a functional ovary and oviduct—may have considerable effects on egg shape (*13*). In particular, such adaptations place constraints on the maximum size or width of a stretched oviduct, which in turn can be accommodated by increasing ellipticity and/or asymmetry of eggs to increase egg volume while maintaining or reducing girth. In accordance with this idea, we find that for a given girth (the widest part of the egg), species laying eggs that are more asymmetric (Fig. 5A) or more elliptical (Fig. 5B) tend to possess eggs that have higher volumes.

We do not suggest that a female's flight behavior during the egg formation period directly affects egg formation, nor do we suggest that egg shape so strongly influences the flight abilities of female birds during their egg-laying period that selection has produced an aerodynamic egg. Rather, we propose that general adaptations for strong flight select for a constrained, muscular, streamlined body plan in both males and females, giving rise in the latter, directly or indirectly, to asymmetric and/or elliptical eggs. The precise physiological mechanisms by which morphological adaptations for flight might affect egg shape are unknown. However, the answer most likely lies in the two parameters highlighted by our biophysical model: egg membrane thickness variations and the differential pressure applied across the membrane, both of which are potentially shaped by selection for a streamlined body plan.

Exploring the effect of flight adaptations on egg shape

Why different avian groups take different evolutionary paths (increased asymmetry, ellipticity, or both) toward maintaining or reducing girth is unclear, but considering the deeper evolutionary history of egg shape may yield some insights. We note that some theropod dinosaurs, particularly the maniraptorans from which birds descended, laid asymmetric eggs (*30*). The loss of a functional ovary and oviduct likely occurred near the maniraptoran-avian transition (*30*, *31*) and may be an innovation unique to birds (*32*). Thus, egg asymmetry and the loss of a functional ovary appeared around the same time as, and are perhaps closely linked to, the emergence of powered flight. Egg ellipticity, by contrast, appears to have originated much earlier in reptiles (crocodilians have elliptical eggs, for example), and may have evolved to accommodate the large egg volumes required for precocial offspring, when egg girth is limited by the oviduct or pelvic opening (*31*).

When it comes to powered flight, does egg asymmetry offer added advantages over ellipticity, or is it a consequence of new and extreme morphological shifts, like oviduct loss? The answer remains unknown. However, if asymmetry is physiologically linked to powered flight, we might expect reduced flight-related selection pressure to be associated with less asymmetric egg shapes. Consistent with this hypothesis, we find that kiwis lay hyperelliptical eggs with relatively low asymmetry and that the other flightless ratites lay eggs that are roughly spherical (ostrich) or elliptical without a high degree of asymmetry (rheas and cassowaries) (fig. S13). Contrary to this hypothesis, however, we note that not all flightless birds have evolved symmetric eggs. Penguins are a clear exception (fig. S13), but because they are powerful underwater swimmers, it remains plausible that selection for a streamlined body plan has nonetheless influenced the evolution of egg asymmetry in the absence of flight.

Having found a strong association between HWI and egg shape on a broad taxonomic scale (across all avian orders), we next explored whether these relationships, or others, describe egg-shape variation within smaller avian groups with contrasting life histories and ecologies. First, we compared asymmetry (Fig. 5C) and ellipticity (Fig. 5D) of species with high (upper 50%) HWI versus low (lower 50%) HWI within the 12 most speciose orders in our data set. Although we did not control within orders for phylogeny and other factors, these pairwise comparisons are nonetheless broadly matched for phylogeny by comparing within orders. The results reveal considerable variation among orders in the extent to which asymmetry and ellipticity may vary as a function of HWI but also highlight the generality of the pattern detected in our broad taxonomic analyses (Fig. 5, C and

D, and fig. S14). Specifically, increased HWI (and hence dispersal ability) is generally associated with an increase in both egg asymmetry and ellipticity within orders.

Next, we reran phylogenetic models restricted to (polyphyletic) seabirds (*13*) (table S3), (monophyletic) passerines (order Passeriformes) (table S4), and (monophyletic) shorebirds (order Charadriiformes) (table S5). The results reveal that some additional explanatory variables can contribute to egg-shape variation in particular case studies. For example, in Charadriiformes, variation in egg asymmetry is associated with developmental mode (table S5B and fig. S15) rather than variation in HWI (fig. S14C), perhaps because highly asymmetric eggs can accommodate a pore-dense respiratory site for rapid neural development in precocial chicks (*8*). In Passeriformes, species are more likely to lay elliptical eggs if they have small clutches, after controlling for other effects (table S4C). Thus, life history traits may have a substantial secondary influence on egg-shape evolution on smaller taxonomic scales, but we still find little evidence for the role of cliff-nesting or clutch size in driving the evolution of egg asymmetry, even in the specific groups that inspired these classical hypotheses (seabirds and shorebirds, respectively). Overall, our results suggest that egg shape is largely influenced by morphological traits associated with flight ability, both in Passeriformes (the most speciose avian radiation) (table S4) and across all birds (table S2). However, these associations do not apply equally to all smaller clades (Fig. 5, C and D, and fig. S14), and further research is required to examine egg-shape variation at a range of taxonomic levels.

Conclusions

Avian eggs provide a simple but powerful system in which to explore the physical and evolutionary drivers of morphological diversity. We have shown that a 2D morphospace captures the range of egg shapes produced by birds and that a biophysical model can explain this diversity, with testable predictions linking membrane properties to shape. Our macroevolutionary analyses suggest that birds adapted for high-powered flight may maximize egg size by increasing egg asymmetry and/or ellipticity, while maintaining a streamlined body plan. Moving forward, it will be important to determine how the developmental process of egg shaping is coupled, in terms of physiology and genetics, with evolutionary constraints associated with flight strength and efficiency. A starting point may be to demonstrate whether anatomical features, like pelvic width, are correlated with egg size and HWI.

REFERENCES AND NOTES

1. P. M. Sander, *Science* **337**, 806–808 (2012).
2. M. E. Hauber, *The Book of Eggs* (Univ. of Chicago Press, 2014).
3. T. Birkhead, *The Most Perfect Thing: Inside (and Outside) a Bird's Egg* (Bloomsbury Publishing, 2016).
4. N. G. Smith, *Ibis* **108**, 68–83 (1966).
5. Z. Barta, T. Szekely, *Funct. Ecol.* **11**, 656–662 (1997).
6. J. Hutchinson, *Biol. J. Linn. Soc. London* **70**, 161–187 (2000).
7. A. G. Gosler, J. P. Higham, S. J. Reynolds, *Ecol. Lett.* **8**, 1105–1113 (2005).
8. I. Smart, in *Egg Incubation: Its Effects on Embryonic Development in Birds and Reptiles*, C. Deeming, Ed. (Cambridge University Press, New York, 1991), pp. 101–116.
9. T. R. Birkhead, J. E. Thompson, D. Jackson, J. D. Biggins, *Ibis* **159**, 255–265 (2017).
10. J. B. Iverson, M. A. Ewert, in *Egg Incubation: Its Effects on Embyonic Development in Birds and Reptiles*, C. Deeming, Ed. (Cambridge University Press, New York, 1991), pp. 87–100.
11. D. Baker, *Auk* **119**, 1179–1186 (2002).
12. F. W. Preston, *Auk* **70**, 160–182 (1953).
13. Materials and methods are available online as supplementary materials.
14. D. K. Zelenitsky, *J. Paleontol. Soc. Korea* **22**, 209–216 (2006).
15. N. López-Martínez, E. Vicens, *Palaeontology* **55**, 325–339 (2012).
16. D. C. Deeming, M. Ruta, *R. Soc. Open Sci.* **1**, 140311–140311 (2014).
17. J. R. G. Bradfield, *J. Exp. Biol.* **28**, 125–140 (1951).
18. M. T. Hincke *et al.*, *Front. Biosci.* **17**, 1266–1280 (2012).
19. K.-M. Mao, F. Sultana, M. A. R. Howlider, A. Iwasawa, N. Yoshizaki, *Zoolog. Sci.* **23**, 41–47 (2006).
20. A. Mallock, *Nature* **116**, 311–312 (1925).
21. D. W. Thompson, *On Growth and Form* (Cambridge Univ. Press, 1942).
22. J. Okabe, *Rep. Res. Inst. Appl. Mech.* **1**, 7–30 (1952).
23. E. A. Evans, R. Skalak, *Mechanics and Thermodynamics of Biomembranes* (CRC Press, Boca Raton, FL, 1980).
24. A. Goriely, M. Tabor, *J. Theor. Biol.* **222**, 211–218 (2003).
25. D. A. Balch, C. Tyler, *Br. Poult. Sci.* **5**, 201–215 (1964).
26. R. O. Prum *et al.*, *Nature* **526**, 569–573 (2015).
27. W. Jetz, G. H. Thomas, J. B. Joy, K. Hartmann, A. O. Mooers, *Nature* **491**, 444–448 (2012).
28. R. Lockwood, J. P. Swaddle, J. Rayner, *J. Avian Biol.* **29**, 273–292 (1998).
29. S. Claramunt, E. P. Derryberry, J. V. Remsen Jr., R. T. Brumfield, *Proc. R. Soc. London Ser. B* **279**, 1567–1574 (2012).
30. X. Zheng *et al.*, *Nature* **495**, 507–511 (2013).
31. G. Grellet-Tinner, L. Chiappe, M. Norell, D. Bottjer, *Palaeogeogr. Palaeoclimatol. Palaeoecol.* **232**, 294–321 (2006).
32. T. Sato, Y. N. Cheng, X. C. Wu, D. K. Zelenitsky, Y. F. Hsiao, *Science* **308**, 375–375 (2005).

ACKNOWLEDGMENTS

M.C.S. was supported by Princeton University, with additional support from the L'Oréal USA For Women in Science Fellowship, the L'Oréal-UNESCO International Rising Talents Fellowship, the Harvard Society of Fellows, and the Milton Fund. E.H.Y. was supported by Start-Up Grant no. M4081583 from Nanyang Technological University, Singapore. C.S. was supported by the Oxford Clarendon Fund and the U.S.-U.K. Fulbright Commission. Collection of biometric, life history, and environmental data was supported by a Natural Environment Research Council grant (NE/I028068/1) to J.A.T. L.M. was supported by fellowships from the MacArthur Foundation and the Radcliffe Institute. We thank H. Eyster, D. Swindlehurst, and J. Damore for contributing to data collection; C. Cicero and R. Bowie for specimen access, including digitization of the egg collection at the Museum of Vertebrate Zoology, Berkeley (funded by NSF grant 0646475); and the referees for valuable comments. Egg-shape data reported in this paper are included in the supplementary materials. This study was conceived by M.C.S. and L.M. and designed by M.C.S., J.A.T., and L.M.. The digital morphometric analyses and coding were conducted by M.C.S., E.H.Y., and D.A. M.C.S., C.S., and J.A.T. compiled biometric, life history, and environmental data for birds. The phylogenetic comparative analyses were led by C.S. and J.A.T. L.M. linked the projective geometry parameters to the asymmetry-ellipticity morphospace, and L.M. and E.H.Y. constructed and solved the mathematical model for egg shape. M.C.S., J.A.T., and L.M. coordinated the research, and all authors contributed to writing of the manuscript.

SUPPLEMENTARY MATERIALS

www.sciencemag.org/content/356/6344/1249/suppl/DC1
Materials and Methods
Figs. S1 to S16
Tables S1 to S5
Data S1 and S2
References (*33*–*63*)

10 September 2016; accepted 26 May 2017
10.1126/science.aaj1945

Supplementary Materials for

Form, Function and Evolution of Avian Egg Shape

M. C. Stoddard, E. H. Yong, D. Akkaynak, C. Sheard, J. A. Tobias[†], L. Mahadevan[†]

Correspondence to: mstoddard@princeton.edu, lmahadev@g.harvard.edu

[†]These authors contributed equally to this work.

This PDF file includes:

Materials and Methods
Figs. S1 to S16
Tables S1 to S5
References 33-63

Other Supplementary Materials for this manuscript include the following:

Databases S1 to S2 as zipped archives:
Database S1 Egg shape by species.xlsx
Database S2 Figure details.xlsx

Table of Contents:

MATERIALS AND METHODS

Quantifying egg shape

That avian eggs come in a variety of shapes and sizes is well known (*2*, *3*, *33*). A practical challenge to comparative analyses of egg shape has been that egg shape cannot be described with a scalar, and methods for shape quantification have varied widely (*8*, *11*, *34*). One approach involves curve-fitting a power series to the outline of eggs (*8*, *34*). However, this method lacks a closed form equation. Baker (*11*) used methods of projective geometry (*35*, *36*) to develop a simple algebraic equation to fit egg shape. Projective geometry explores relationships that are preserved under projective transformations so that the distinction between points and lines and the notion of parallelism start to disappear and are instead replaced by notions of incidence (whether or not lines, planes and points coincide). Baker shows how the profile of an egg can be determined by mapping a series of geometric sequences of points on lines perpendicular to an oval; eventually a path curve equation for the egg profile can be derived. Just two parameters, lambda λ and tau T, are needed to describe egg shape across a diverse subset of avian species. We chose to use Baker's (*11*) parameters because they are simple and capture egg morphology naturally: λ (related to asymmetry) and T (related to ellipticity). Baker's equation for the path curve of an egg is:

$$y = T(1+x)^{\frac{1}{1+\lambda}}(1-x)^{\frac{\lambda}{1+\lambda}}$$

We wrote a computer program to extract individual eggs from digital images and to fit the Baker equation to each egg, yielding λ and T. This computer program, **EGGXTRACTOR**, is freely available upon request and can be readily applied to diverse questions about egg morphology across taxa.

Digital image processing

We used all available digital images of eggs on the Museum of Vertebrate Zoology (University of California, Berkeley) database. We applied the same standardized, automated shape analysis to all images, and to facilitate this we excluded images taken outdoors, or containing eggs that were either severely cracked or laid by brood parasites. Species information for clutches containing parasitic eggs was sometimes erroneous or missing from the specimen cards, so we discounted any parasitic eggs noted on specimen cards or detected by our own visual inspection to avoid potential misidentifications. The MVZ database included meta-data for images, including information about species, location, date and collector.

We created and applied masks for all eggs in all images and then fit a path curve (*11*) to each individual egg outline (Fig. S1). The path curve is defined by two independent parameters: lambda λ and tau T (see previous section). In practice, we found that $\lambda \in [1,2)$ and $T \in [0,1)$ account for the avian egg shapes we see in nature. All images contained a scale bar so we were

also able to extract the length of the major axis (in centimeters) for each egg. We also measured egg girth, the widest/fattest part across (not around) each egg (in centimeters). Each MVZ image contained one clutch of eggs; we obtained the average lambda, tau, length and girth for each clutch. These average per-clutch values were later used to calculate the species averages for asymmetry and ellipticity (see below).

For highly symmetric eggs ($\lambda \approx 1$), our algorithm occasionally computed λ values slightly less than 1 due to the nature of the numerical computation process. However, there is a one-to-one map between an egg with Baker parameters (λ, T) and another egg with Baker parameters $(1/\lambda, T)$, the difference being whether the pointed end of the egg is oriented to the left or to the right. To ensure consistency in our dataset, we oriented all eggs such that the pointed end was always to the right. This reduced our domain space to $\lambda \in [1, \infty)$ and $T \in (0, \infty)$.

A more natural set of variables transforms λ and T to A (asymmetry) and E (ellipticity), respectively. Since we were interested in measuring deviation away from the symmetric spherical egg, $(\lambda, T) = (1,1)$, we defined two new scaled parameters: asymmetry $A = \lambda - 1$ and ellipticity $E = \frac{1}{T} - 1$, so that $A \epsilon [0, 1)$ and $E \in [0, \infty)$, so that a symmetric spherical egg is $(A, E) = (0, 0)$.

We also followed Baker (*11*) in calculating the regression error ϵ, which is used to determine how much the fitted curve deviates from the actual egg outline. We define ϵ explicitly as:

$$\epsilon = \sum_{i=1}^{n} \left(\frac{r_{actual,i}}{r_{actual,eq}} - \frac{r_{synth,i}}{r_{synth,eq}} \right)^2$$

where n is the number of discrete points on the egg outline, subscripts *actual* and *synth* refer to the actual egg's contour and the synthesized egg's contour respectively, and *eq* denotes the equatorial radius of the egg. Eggs were eliminated if $\epsilon > 0.01$. A plot of the shape parameters of all eggs that were kept and eliminated (~3% total) is shown in Fig. S2. The plot reveals that the Baker equation for a path curve sometimes fails to provide a good fit for extremely pointy/asymmetric eggs. We note that eliminating eggs that failed the "goodness-of-fit" test described above does slightly constrain the apparent variation in egg shape. Therefore, our morphospace is conservative in its demonstration of variation.

After eliminating eggs with poor curve fits, we had 49,175 eggs from 13,049 images, representing ~1400 avian species from 37 orders. A list of these species is included in Database S1. For attributing species names and order names, we followed the taxonomy described on BirdTree (*27*). We note that our list includes a few species which are sometimes treated as subspecies. These include *Gallinago (gallinago) delicata* and *Gallinago (gallinago) gallinago*,

Porphyrio (porphyrio) madagascariensis and *Porphyrio (porphyrio) poliocephalus*, *Junco (hyemalis) bairdi*, *Junco (hyemalis) caniceps*, *Junco (hyemalis) hyemalis* and *Junco (hyemalis) oreganus*, *Carduelis (flammea) cabaret* and *Carduelis (flammea) flammea*, *Synallaxis (azarae) azarae* and *Synallaxis (azarae) superciliosa*, and *Rhipidura (albicollis) albicollis* and *Rhipidura (albicollis) albogularis.* The parent species is given in parentheses. We treated the above examples as separate species in the morphospace analyses but we followed the Jetz et al. (*27*) designation in the comparative analyses. Family assignment was obtained from the Handbook of the Birds of the World Alive (www.hbw.com) on 31 March 2017. An R script was used to automatically record the family from the species whose HBW Alive webpages matched the scientific and English names given in the BirdTree (*27*) taxonomy (955 of 1396); the remaining families were searched by hand.

Morphospace analyses

Egg shapes range from $A = 0.001$ (*Streptopelia bitorquata*, Island Collared Dove) to 0.485 (*Calidris minutilla*, Least Sandpiper) and $E = 0.097$ (*Ninox scutulata*, Brown Hawk-owl) to 0.724 (*Macrocephalon maleo*, Maleo) (Fig. 1). Missing from the occupied morphospace are eggs that are both fairly spherical (fatter, less elliptical) and asymmetric (with a pointed end) (Fig. S3). We identified the most common avian egg shape: a density map (Fig. S4) reveals that, among our ~1400 species, many species converge on egg shapes falling between $A = 0.1 - 0.2$ and $E = 0.3 - 0.4$, similar in shape to the egg of the Graceful Prinia (*Prinia gracilis*) (Fig. 1). A total of 167 species (~12% of our sample) fall in the seven densest hexagonal bins in morphospace (out of 352 possible bins, or 2%). The hexagonal bin with the greatest density includes eggs laid by 26 species in 16 families and 3 orders, with an average $A = 0.13$ and $E = 0.31$.

We determined that the avian orders with the 8 largest areas in the two-dimensional morphospace are: Charadriiformes, Passeriformes, Galliformes, Accipitriformes, Procellariiformes, Apodiformes, Anseriformes and Gruiformes (Fig. S7, Table S1). One caveat is that the orders occupying large portions of the shape space also tend to contain high numbers of representative species; morphospace occupancy is highly correlated with the number of sampled species per order (Table S1). However, our sampling effort is moderately correlated with the real number of species in each order, so our sample provides a rough approximation of the natural shape variation in each clade.

We also compared the egg shape morphospace of birds to the egg shape morphospace of theropod dinosaurs, non-avian reptiles and mammals (Fig. S8B), using data from (*16*) and (*15*). To perform the conversion of the egg shapes described in (*16*), we used their equations for deriving the elongation ratio (ER) and the asymmetry ratio (AR) and applied them to all of the eggs in our dataset. This allowed us to derive a linear transformation from the ER/AR space to our asymmetry/ellipticity space, which we then applied to the eggs in (*16*). To analyze the eggs described in (*15*), we used the shape profiles in their Figure 7 to extract our asymmetry and

ellipticity values directly. In Fig. S8B, the extant bird egg with very high asymmetry is a *Uria* (murre or guillemot) egg (*15*); this particular egg (but not all *Uria* eggs) would have failed our goodness-of-fit test. Eggs with ellipticity > 1 are not shown in the figure, including from (*16*) some snakes, crocodiles, non-avian theropod dinosaurs, and Mesozoic birds; and from (*15*) some non-avian theropod dinosaurs. We note that egg shape comparisons among non-avian vertebrates should be considered preliminary because few non-avian theropod dinosaur eggs have been described.

In addition, we show how our egg shape morphospace differs from that of Baker (*11*) (Fig. S8A). Several eggs with very high asymmetry appear in Baker's morphospace but not in our own. We show all of the eggs in the Baker dataset (red dots), even those with a poor curve fit, whereas, for our egg data (black dots), we plot only the eggs in our final dataset (after eliminating eggs with poor curve fits – see Fig. S2). Finally, in addition to plotting eggs in a two-dimensional morphospace, we also visualized the space with a third dimension, egg length (Fig. S6).

Biophysical model

Mallock (*20*) proposed that the walls of the isthmus may be differentially elastic, so that the application of pressure within the oviduct could thus generate a wide variety of egg shapes. If this alone were the case, the egg would revert to becoming spherical once the shell is removed. Given that this does not happen (*17*), we must rule out this explanation. Okabe (*22*) subsequently suggested that egg shape results from pressure from the wall of the oviduct, peristaltic motion as the egg is thrust down the oviduct, and friction between the egg and oviduct but did not account for how the eggshell membranes affect egg shape. Again, the fact that shell removal does not change the egg's shape contradicts the view that pressure/motion/friction alone explain egg shaping. Subsequently, Smart (*8*) posited that muscular action in the isthmus is likely to affect egg shape.

Our proposed model starts with the simplest hypothesis consistent with a non-spherical shape for a pressurized closed elastic membrane: that the membrane properties are inhomogeneous as one traverses from pole to pole, *i.e.* along the axis of the oviduct. In addition, differential pressure can be applied across the eggshell membrane. We do not specify how differential pressure arises – it could arise from differential elasticity of the isthmus wall, water absorption ('plumping'), muscular contraction, or some combination of these – but the end result is that inhomogeneous variation in the properties of the eggshell membrane (actually a double membrane, but we refer to it here as a single membrane for clarity) and in the pressure across the egg's surface can give rise to different egg shapes.

The fundamental details of the model are summarized in the main text and in Fig. 3. We note that this type of approach has been used successfully to illustrate elastic membrane growth in other contexts (*24*), and we adapt it here to describe the process of egg shape formation. The shape of

an axisymmetric egg can be completely described by a planar curve C and characterized by a curve with radial and angular coordinates $[r(\sigma), \theta(\sigma)]$ as a function of a curvilinear material coordinate σ (Fig. 3). We can define the axial (longitudinal) extension ratio $\lambda_s = \partial s/\partial\sigma$, where *s* is the stretched coordinate, and the azimuthal (radial) extension ratio $\lambda_\varphi = r/r_0$. We can also define the associated principal strains $e_{ss} = \frac{\lambda_s^2-1}{2};\ e_{\varphi\varphi} = \frac{\lambda_\varphi^2-1}{2}$ and, assuming a simple linear constitutive relation linking stress and strain (*23*), we can write the depth-integrated (or thickness-integrated) axial and azimuthal stresses as $t_s = A(\sigma)e_{ss} + B(\sigma)e_{\varphi\varphi}; t_\varphi = A(\sigma)e_{\varphi\varphi} + B(\sigma)e_{ss}$, where $A(\sigma), B(\sigma)$ are the depth-integrated axial and azimuthal stiffnesses of the egg membrane respectively. In terms of the principal curvatures of the membrane $\kappa_s = \frac{\partial\theta}{\partial s};\ \kappa_\varphi = \frac{sin\theta}{r}$, the equations of mechanical equilibrium for the surface in the normal and tangential directions can then be written as $P = \kappa_s t_s + \kappa_\varphi t_\varphi;\ \partial(rt_s)/\partial s\ - t_\varphi \partial r/\partial s\ = 0$, where P is the difference in pressure across the membrane and t_s, t_φ are the tensions on the surface along the principal directions (*23*).

There are two functions in the governing equations, the ratio of azimuthal to axial stiffness $\mu(\sigma) = B(\sigma)/A(\sigma)$, and the scaled pressure $p(\sigma) = P/A(\sigma)$, both of which can vary along the membrane coordinate σ. In the simplest case, $A(\sigma) = cEh(\sigma), B(\sigma) = dEh(\sigma)$, where E is the Young's modulus, $h(\sigma)$ is the wall thickness of the deformed membrane and c, d are dimensionless constants. If $\mu(\sigma), p(\sigma)$ are constant, the curve would be a semi-circle and the membrane would be a simple symmetric sphere (Fig. S9B). As $\mu(\sigma), p(\sigma)$ become non-trivial functions of the material coordinate σ, the shape will become aspherical (elliptical) and asymmetric (Fig. S9E). We assume that the pressure difference P is constant across the membrane, *i.e.* there are no effects associated with fluid flow and the system is in elastic and hydrostatic equilibrium. Consequently, variation in the scaled pressure $p(\sigma) = P/A(\sigma)$ is solely due to variations in $A(\sigma)$ (the axial stiffness of the egg membrane). Decreased axial stiffness or increased pressure are functionally identical owing to the fact that they appear only as a ratio in the governing equations; similarly, only the ratio of azimuthal to axial stiffness appears in the scaled governing equations.

Writing the axial extension ratio as

(1) $\lambda_s^2 = 1 + \mu\left(1 - \left(\frac{r}{r_0}\right)^2\right) + \frac{rp}{2sin\theta}$, we obtain a closed system for the variables $\big(r(\sigma), \theta(\sigma)\big)$, which are given by (*23*, *24*):

(2) $\frac{\partial r}{\partial\sigma} = \lambda_s cos\theta;\ \frac{\partial\theta}{\partial\sigma} = -\left(\frac{\lambda_s}{r}\right)\frac{sin\theta\left[r^2 - r_0^2\left(1+\mu\left(1-\lambda_s^2\right)\right)\right] - prr_0^2}{r^2\mu - r_0^2(1+\mu-\lambda_s^2)}$.

When coupled with the auxiliary relations:

(3) $\frac{\partial z}{\partial \sigma} = \lambda_s sin\theta; \frac{\partial s}{\partial \sigma} = \lambda_s,$

this set of equations describes the deformation of a stretchable axisymmetric elastic membrane defined relative to the reference shape $r_0(\sigma)$, once we prescribe the functions $\mu(\sigma), p(\sigma)$ that characterize the axial/azimuthal elastic anisotropy of the membrane, and the scaled pressure that deforms it. To complete the formulation of the problem, we also prescribe the following boundary conditions over the domain $\sigma \in [0, L_0]$, where L_0 is the total longitudinal length of the unstretched membrane: $r(0) = 0; r(L_0) = 0;\ \theta(0) = 0; \theta(L_0) = \pi$.

Asymmetric, elliptical shapes result from nonuniformity in $\mu(\sigma), p(\sigma)$. When $\mu(\sigma), p(\sigma)$ are constant, the egg is spherical. An egg can become asymmetric if $\mu(\sigma)$ or $p(\sigma)$ does not vary symmetrically across the egg's midpoint. In an asymmetric egg, the scaled pressure can be high at the pointy end of the egg and low at the blunt end of the egg, where the membrane thickness (or stiffness) is high. From a sphere, an egg can become elliptical if $\mu(\sigma)$ or $p(\sigma)$ is no longer constant but varies symmetrically across the egg's midpoint, such that stretching occurs more in the axial direction than in the azimuthal direction.

In order to incorporate a growth mechanism for egg shapes, we use an iterative approach that is commonly used to incorporate growth into elastic descriptions (*24*, *37*, *38*). This procedure is a quasi-static discrete growth process as illustrated in Fig. 3. We start with an initial shape defined by the function $r_0(\sigma), 0 \leq \sigma \leq L_0$ and compute the new equilibrium shape $r(\sigma)$ by solving the boundary value problem as described above. The new shape $r(\sigma)$ represents the new mechanical equilibrium of the membrane based on the prescribed $\mu_0(\sigma), p_0(\sigma)$. The effect of growth is achieved by setting this new shape $r(\sigma)$ as a new reference shape in the next step of iteration: $r_1(\sigma) = r(s), 0 \leq \sigma \leq L_1$, where s is the arc length along the stretched curve with total longitudinal length L_1. The shape $r_1(\sigma)$ is then used to solve the boundary value problem with parameters $\mu_1(\sigma), p_1(\sigma)$ over the new domain $0 \leq \sigma \leq L_1$. We may iterate this discrete growth process to the desired number of steps N to get the final shape $r_N(\sigma)$. From the final equilibrium shape, after a simple rescaling of the egg by its major axis length L, we can calculate the rescaled Baker (*11*) parameters (A, E).

We solve the nonlinear equations for the shape of the egg given above numerically using MATLAB using two different sets of $\mu(\sigma), p(\sigma)$. For eggs that have average values of asymmetry (A~0.2) and ellipticity (E~0.5), we find that using a simple power law $p(\sigma) = (\sigma + a)^{-b}$, $\mu(\sigma) = c$, where *a,b,c,* are positive real numbers, can generate the majority of real egg shapes within N=5 growth steps. Typical values are *a~0.3, b~2, c~0.5.* In principle, the phenomenological parameters $\mu_i(\sigma), p_i(\sigma)$ may change during each growth step $i = 1, \dots, N$. In practice, we find that using the same functional form during each step suffices to generate the egg morphospace. The functional form (the simple power law above) is by no means unique, and

using other smooth functions yields similar results. Most of the growth of the initial circular egg is concentrated at one end of the egg where the scaled pressure is very high. This is due to the membrane being much thinner at that particular end. This scaled pressure profile can generate shapes that are asymmetric and elliptical (Fig. S9).

By adding a small asymmetry in $\mu(\sigma) = c + d \tanh[e(\sigma - f)]$, where d, e, f are positive real numbers, we can get highly asymmetric egg shapes ($A > 0.4$) using a given power law expression for $p(\sigma)$. In this case, the asymmetry in $\mu(\sigma)$ enables us to generate highly asymmetrical egg shapes. Overall, we show that our simple biophysical approach can capture the basic achieved morphospace of egg shapes (Fig. 3E).

In addition, our model can generate counterfactual eggs that are not found in nature (Fig. S10). We find that these counterfactual eggs are generated when we introduce sudden variations in pressure/thickness/inhomogeneity. For example, using the following functional forms, $p(\sigma) = (\sigma + a)^{-b}$, $\mu(\sigma) = c + d \tanh[e(\sigma - f)]$ (see Fig. S10 for details) for different growth steps, we can generate the unusual shapes shown in Fig. S10. From these counterfactual eggs, we hypothesize that living birds do not have rapid variations in membrane properties; otherwise we would expect to see such shapes in nature. Alternatively, microscopic manipulations during egg formation that change the membrane properties might lead to abnormal morphologies, which are typically selected against. Whether the lack of counterfactual egg shapes in nature stems from mechanistic constraint or natural selection requires further study. Not surprisingly, the simple projective geometry approach embodied in the Baker equation does not provide a particularly good fit to these counterfactual egg shapes; nonetheless, the biophysical model, which correctly accounts for both geometry and mechanics, is capable of generating them.

Our model naturally raises the question: if we know the shape of the egg, what can we deduce about its membrane properties and pressure? This is an inverse problem, which is difficult in general (mathematically, it is ill-posed, as there are many combinations of thickness and moduli that can all give rise to the same egg shape). Our model does not make absolute predictions, but it does provide relative information. For example, for an egg with values of asymmetry (A~0.2) and ellipticity (E~0.5), we find that a simple power law, $\mu(\sigma) = \frac{1}{2}, p(\sigma) = (\sigma + a)^{-b}$, where a, b are positive real numbers, can generate the real egg shape within 5 growth steps. From our numerical testing, we find that if the thickness is simply inversely proportional to the scaled pressure, *i.e.* $h(\sigma) = (\sigma + a)^b$, the posterior end (the blunt end) of the egg membrane is much thicker than the anterior end (the pointed end), the result of which is that this (blunt) end will have a smaller curvature. The thinner part of the membrane, at the pointed end, experiences greater stretching. See Fig. S9 for further details. While our model can capture the qualitative trends seen in nature, to go beyond this requires the detailed description of how these physical parameters (membrane thickness, elasticity and pressure) vary across living birds (and their relatives), likely through detailed histological analysis of the oviduct and membranes, *in situ*

pressure measurements, and MRI scans of live birds during the process of egg formation.

What empirical evidence is there to suggest that our model is plausible? Membrane thickness of chicken eggs appears to vary considerably across the shell's latitude (*25*), such that the thinnest part is ~65% of the thickest part, as shown in Fig. 3C. In addition, the fiber diameters of the chicken egg membrane become larger as you move from the inner membrane to the outer membrane, which could affect stiffness properties (*39*). The pressure, which may arise from differential elasticity of the isthmus wall, water absorption ('plumping'), muscular contraction, or some combination of these, could be applied according to a power law, as a function of sigma (location), such that some parts of the egg would receive more pressure than others.

Could egg stiffness and strength impose constraints on egg shape? Recent work (*40*, *41*) showed that the rigidity at the pole of a synthetic ellipsoidal membrane increases with asymmetry. This suggests that if there is an evolutionary requirement for the egg membrane to develop a maximally stiff location, then the egg will become more asymmetric. However, this also leads to a relative weakening of the strength of the membrane at the equatorial part of the egg. For an egg that needs to be isotropically stiff and tough, the best shape to adopt would be a spherical shape. Future work should explore the mechanical demands of the eggs, in terms of incidental damage at the nest (bumping into other eggs, force from the incubating parent) and hatch behavior to determine whether there are links between egg shape and diverse structural requirements at the nest.

Phylogenetic comparative methods

Life history and environmental parameters

We compiled a dataset with biometric, life history and environmental parameters for all species in our sample, including information about clutch size, nest type, nest location, diet, adult body mass, adult hand-wing index, and chick developmental mode (*e.g.* precocial). We also compiled data on spatial location or environmental conditions (*e.g.* latitude, temperature and average precipitation) extracted from geographical range polygons. Clutch size information was obtained from (*42*) and from the online Handbook of the Birds of the World Alive (*43*). We also used Handbook of the Birds of the World Alive to compile information on nesting behavior, which we scored in terms of nest type (scrape, plate, or cup) and nest location (non-cavity ground, non-cavity elevated, cavity).

Using published information (*44*), we assigned all species to three dietary categories where 0 = herbivorous, 1 = a mixture of plant and animal diets, and 2 = carnivorous. Herbivores were defined as species consuming solely plant material, including leaves, buds, fruit, seeds and nectar. Carnivores were defined as species consuming only animal prey, including all vertebrates, arthropods, arachnids, molluscs, and other marine groups. For species with low proportions (10%) of animal or plant food in the diet, we verified our classification by checking

the literature (HBW Alive, http://www.hbw.com/). This led to a few cases where we reclassified species as herbivores if they ate animal material only very rarely, or as carnivores if they only ate plant material only very rarely. We assumed that the calcium content of the diet increased from purely herbivorous diets to purely carnivorous diets.

For each study species we also collected wing measurements from field collections (5%) and preserved museum skins (95%). Following Claramunt et al. (*29*), we computed hand-wing index (HWI) as the ratio of Kipp's distance (distance between the tip of the longest primary/wing tip and the first secondary feather) to total wing chord (distance between the carpal joint to wing tip), both measured on the folded wing with primaries unflattened. Where possible, we obtained measurements from at least 4 individuals (2 from each sex) for each species (n = 6302 specimens, mean = 4.52 per species), following standard protocols (*45*, *46*).

Kipp's distance and HWI are measures of wing-tip shape, providing information about the narrowness and pointedness of the avian wing. Previous analyses have shown that Kipp's distance predicts natal dispersal distance (*47*), while both Kipp's distance and HWI are related to migratory behavior (*28*, *29*, *48*, *49*). Nonetheless, we argue that neither dispersal nor migration really captures the essence of flight ability because, for example, many species spend enormous amounts of time in flight despite being non-migratory with very low dispersal (*e.g.* shorebirds, hummingbirds). We suspect that wing-tip shape captures variation in avian flight ability much better than previous studies imply because species with stronger and more frequent flight tend to have narrower and more pointed wing-tips, whereas species with weaker and less frequent flight tend to have shorter, more rounded wingtips. We chose to use HWI as a proxy for flight ability in our analyses because it is scaled to wing length and provides a better approximation of wing aspect ratio (WAR) (*29*, *49*). WAR is an index of fundamental aerodynamic properties of wing shape that are correlated with flight efficiency and the propensity for sustained flight in volant animals (*50*, *51*). For this reason, HWI has become the standard index of avian dispersal ability used in comparative analyses (*29*, *45*, *46*, *52*). We also note that HWI is highly correlated with Kipp's distance: accounting for body mass variation, and controlling for shared ancestry with phylogenetic correction, the two metrics are strongly associated in our dataset (estimated model $R^2 = 0.619$, $p < 0.001$).

To estimate WAR, we use HWI because it can be measured from dried museum specimens whereas WAR can only be measured directly on live or freshly killed birds. We acknowledge that bird wings and other body parts shrink over time in museum specimens, but this is not thought to affect our calculation of HWI because the relative level of shrinkage is generally tiny (*53*). Moreover, as HWI is a ratio, any specimen shrinkage is likely to affect Kipp's distance and wing chord in equal proportion and thus to preserve the HWI. To check this, we ran a linear model on a database of over 40,000 HWIs from over 10,000 species of birds (JAT, unpublished data) and found no statistical differences between museum and field measurements.

Chick developmental mode was scored in eight categories 1-8 (superprecocial, precocial 1, precocial 2, precocial 3, semiprecocial, semialtricial, altricial 1, altricial 2), following (*54*). Adult body masses were obtained from (*55*) and log-transformed. Finally, species-level range median latitude along with mean temperature and precipitation from the Worldclim database (*56*) were calculated from global range polygons (BirdLife International 2011, *Bird species distribution maps of the world*. Cambridge, UK, Nature Serve, http://www.birdlife.org/datazone/info/spcdownload).

These life history and environmental parameters were used as predictive variables in our phylogenetic models (see following sections). Note that we included both adult body mass and egg length as predictor variables in our models even though these are highly correlated (linear regression with both variables log-transformed, $R^2 = 0.91$), as we have *a priori* hypotheses suggesting that both variables relate to egg shape and as we have a large enough sample size to accurately estimate both coefficients. To control for this collinearity, however, we ran a phylogenetically-controlled principal components analysis (*57*) on the two log-transformed variables. Thus, body mass and egg length were together represented by the first principal components axis PC1, an overall measure of the egg's size, and by the second axis PC2, a measure of whether the egg is longer (positive PC2) or shorter (negative PC2) than expected given the bird's body mass.

PC1 and PC2 are important because they help clarify the relationships we find with flight ability (HWI). Flight ability is correlated with high degrees of egg asymmetry and ellipticity. We suggest that as an adaptation for more efficient flight, birds reduce their body size and otherwise streamline their body plans, including the oviduct. Thus, birds accommodate their greater aerodynamic needs by laying eggs that maximize volume while maintaining (or reducing) girth and thus lay eggs that are asymmetric and elliptical. At a broad taxonomic level, birds lay eggs that are more asymmetric if they have high HWI and/or if they have large eggs/large body mass (high PC1), controlling for other effects. Birds lay eggs that are more elliptical if they have high HWI and/or large eggs/large body mass (high PC1) and/or large eggs for a given body size (high PC2), controlling for other effects (and we note also that diet had a marginally significant effect). Thus, high egg ellipticity is generally associated with larger eggs/larger body size, but it may be most advantageous for birds that lay large eggs for their body size. For these birds, elliptical eggs may help solve the problem of producing a large egg in a small body streamlined for flight.

We chose to use egg length in our analyses rather than egg volume. We did this because we were able to measure length directly from the 2D photographs in our dataset, whereas our 3D volume measurements were estimates, following an equation derived by Baker (*11*), such that:

$$V = \frac{\pi L^3}{8} \int_{-1}^{1} y^2 dx$$

where L is the actual length (in cm) of the egg and y is the the Baker equation for the path curve of an egg. Thus, there is a cubic relationship between volume and length for a constant shape. However, given that egg shape is related to egg length, and that we are working with relatively small lengths, the relationship between log(volume) and log(length) is very close to linear (Fig. S16).

Because of the tight correlation between length and volume, we did not expect the results of the phylogenetic modeling to change when we substituted volume for length; moreover, due to the high collinearity of volume and length, it is best to use one or the other but not both measurements in the statistical models. Indeed, when we repeated the phylogenetic analyses using volume instead of length, we observed no meaningful differences.

Tree acquisition

100 randomly-selected phylogenetic trees were obtained from the Hackett backbone of the Global Bird Tree (*27*), restricted to the 1209 species for which there exists known genetic data – hereafter called "Jetz trees" – and complete macroecological data. To account for more recent information on deep-time phylogenetic relationships among birds, we also obtained the 198-species tree published in (*26*): hereafter called the "Prum backbone." Only 65 of our 1209 species were in this Prum backbone, so we sought to add our remaining 1144 species to it using more recent phylogenetic information from the Jetz trees. For each Jetz tree T_i, we found the nearest phylogenetic relative within T_i that was also present on the Prum backbone. We then added that species to the Prum backbone along the lineage containing that nearest relative, at the time at which those two species diverged in the Jetz tree. The 133 lineages on the Prum backbone not in our dataset were removed at the end of this procedure. The 100 resultant trees are referred to as the "Prum trees."

Phylogenetic tests

All phylogenetic analyses were performed twice: once on the Jetz trees and once on the Prum trees (see above). Both tree topologies yielded similar results, but in the main paper we generally present the results based on the Prum tree, as this contained the most comprehensive dataset in terms of genetic loci. We used these trees as a framework for performing Bayesian mixed-effect models with Gaussian error and phylogeny as a random effect, using a Markov-chain Monte Carlo algorithm, implemented in the *R* package MCMCglmm (Markov chain Monte Carlo generalized linear mixed models) (*58*). Each model was run for a total of 5,500,000 iterations with the first 500,000 iterations discarded as burn-in and sampling every 5,000 iterations, constrained such that 55,000 iterations with a burn-in of 5,000 would be run on each of 100 trees. All continuous variables were rescaled to have a mean of 0 and a variance of 1 so as to be

directly comparable, and plots of the sampled output were visually inspected to check model convergence and to ensure proper mixing.

We performed phylogenetic models using the entire tree and also, to test the generality of our findings, within specific ecological groups and clades: (polyphyletic) seabirds (Table S3), (monophyletic) passerines (Table S4) and (monophyletic) shorebirds (Table S5). To define seabirds, we followed Wilman et al. 2014 (*44*) in considering pelagic specialists to include some Anseriformes (2 species in Anatidae), some Charadriiformes (all species in Alcidae, some species in Stercorariidae, some species in Laridae), some Pelecaniformes (1 species in Ardeidae), all Phaethontiformes (all 3 species in Phaethontidae), all Procellariiformes (all species in Diomedeidae, Hydrobatidae, Pelecanoididae, Procellariidae), all Sphenisciformes (all species in Spheniscidae), and some Suliformes (all species in Fregatidae, some Phalacrocoracidae, all species in Sulidae, and no species in Anhingidae).

In passerines, HWI and body mass/egg length (PC1, PC2) affect egg asymmetry – but so do precipitation (marginally) and temperature, with birds nesting in cool localities and/or with high precipitation tending to lay more asymmetric eggs (Table S4-B). In shorebirds, developmental mode (in addition to body mass/egg length PC1) is a predictor of egg asymmetry, with more precocial chicks hatching from more asymmetric eggs (Table S5-B, Fig. S15). In both seabirds and shorebirds, egg ellipticity is predicted by nest elevation (in addition to body mass/egg length PC1), with birds tending to lay more elliptical eggs if they nest in elevated nests (not cavities) (Table S3-C, Table S5-C). In passerines, ellipticity is (marginally) influenced by egg clutch size (in addition to HWI and body mass/length PC1, PC2), with birds more likely to lay elliptical eggs if their clutches are small; however, this was detected only with the Jetz topology and not the Prum topology (Table S4-C). Based on these patterns, it appears that – at a very broad taxonomic level – egg shape in birds is largely influenced by morphological traits, including adult body mass, egg length and HWI (adaptations for flight). However, life history traits can have strong secondary effects, which become clear when we consider specific ecological groups and clades.

In addition, we compared asymmetry and ellipticity within the 12 most speciose orders within our dataset (Fig. 5A, B, Fig. S14), so chosen because we had more than 20 species within each of these orders. By comparing species within orders, we broadly controlled for phylogeny.

Adaptations for flight

We find that, across birds, egg asymmetry is predicted by adult body mass/egg length and HWI, such that birds – for a given egg length and adult body mass – tend to lay asymmetric eggs if they have high HWI (Table S2-B). Similarly, for a given egg length, adult body mass and diet, birds tend to lay more elliptical eggs if they have high HWI (Table S2-C). Given that HWI is related to flight ability in birds (see above), these results give some weight to a little-known

suggestion that the "reduced abdominal space typical of birds (presumably an adaptation for flight, as is the habit of carrying only a single shelled egg at a time), may therefore be the most important determinant of egg-shape in birds" (*10*).

Is there evidence to support the idea that morphological changes associated with flight can affect the process of egg shape formation? One key adaptation for flight involves the evolution of greatly reduced body size (*59*) and a reduced abdominal cavity. Powered flight has huge energetic costs: long-distant migrants exhibit organ reduction after long flights (*60*); over evolutionary time, some birds may have evolved more compact, streamlined body plans as a result. A second adaptation for flight appears to be the loss of one functional ovary and oviduct in modern birds, which reduced body weight and required females to carry only a single egg at a time. Among the amniotes, birds are unusual in that they have a single functional ovary and oviduct (the left one) in the adult, with a few exceptions (the kiwi has two functional ovaries). Non-avian reptiles and mammals, by contrast, possess two ovaries and oviducts. Some theropod dinosaurs laid asymmetric eggs and may have possessed just one functional oviduct (*14*, *15*, *30*, *31*), although there is also strong evidence showing that some maniraptoran species retained two functional oviducts (*32*). Either way, the loss of one functional oviduct appears to have occurred as theropods transitioned to early birds (and indeed could be unique to birds), at the same time early birds acquired flight (*30*, *61*), raising the possibility that egg asymmetry and flight arose around the same time. From a physiological standpoint, if egg asymmetry stems from the application of differential pressure to the egg in the isthmus, possessing a single egg in a single oviduct would allow for more precise control over egg shape than would be possible if two or more eggs were carried in the oviducts simultaneously, as in other reptiles (*10*). Interestingly, loss of an oviduct does not appear to be an essential precursor to powered flight; pterosaurs – which evolved flight earlier, independently – apparently had two functional oviducts (*62*). However, their eggs were small, had thin shells (*62*) and were not highly asymmetric (*16*).

A final observation is that in the isthmus, most bird eggs form such that the leading end (closest to the cloaca) is pointed and the trailing end is blunt; the egg then rotates in the shell gland so that it can be laid blunt-end first. This rotation suggests that egg formation is strongly affected by abdominal shape and oviduct morphology (*10*), so much so that birds have evolved a mechanism for a late-stage rotation of the egg in order for it to be laid blunt-end first, for which there is apparently strong selective pressure. Why selection would favor egg-laying to proceed with the blunt end first is unclear (*3*), however, and several species do not lay eggs blunt-end first, including guillemots (*3*) and some ducks and geese (*63*).

Based on these lines of evidence, we suggest that morphological adaptations for flight – including a streamlined body plan, reduced body size, a reduced abdominal cavity, and a single ovary and oviduct – may have influenced egg shape, such that birds that are highly adapted for flight maximize the egg's size without increasing its girth (width) by increasing its asymmetry

and/or ellipticity (Fig. 5A, B). Thus, a bird can produce a large egg while still retaining an aerodynamic body plan. Overall, a general constraint on body size (and particularly for birds that lay big eggs for their body size, according to our analysis) appears to select for highly asymmetric and elliptical eggs.

Figure S1. Workflow for the import, masking, extraction and curve-fitting of eggs in images.

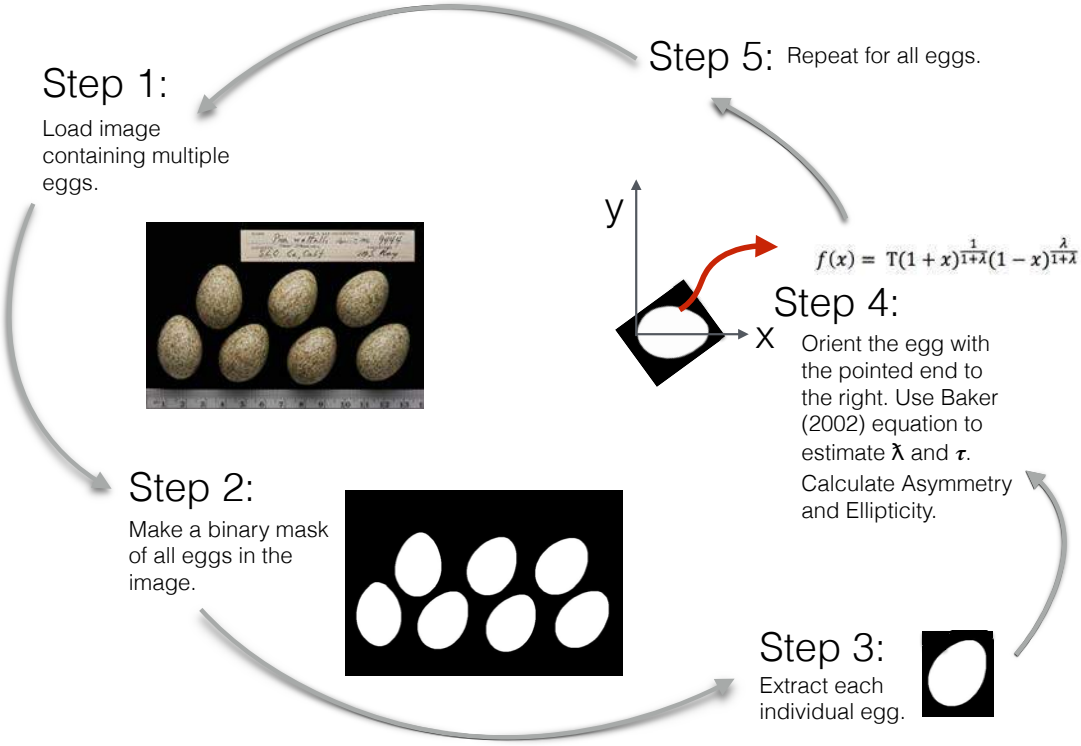

Figure S2. (A) We rejected approximately 3% of all eggs (shown in red, green and turquoise), when the regression error epsilon > .01, based on a goodness-of-fit test. In general, the Baker equation for a path curve fails to provide a good fit for irregular or very pointy/asymmetric eggs. Eliminating these eggs slightly constrains the apparent variation in egg shape, and our morphospace is therefore conservative in its estimate of variation. Eggs not rejected (the 49,175 in the final dataset) are shown in black. **(B)** The fit of Baker's egg shape equation declines as epsilon increases. The value of epsilon is shown inside each egg.

A

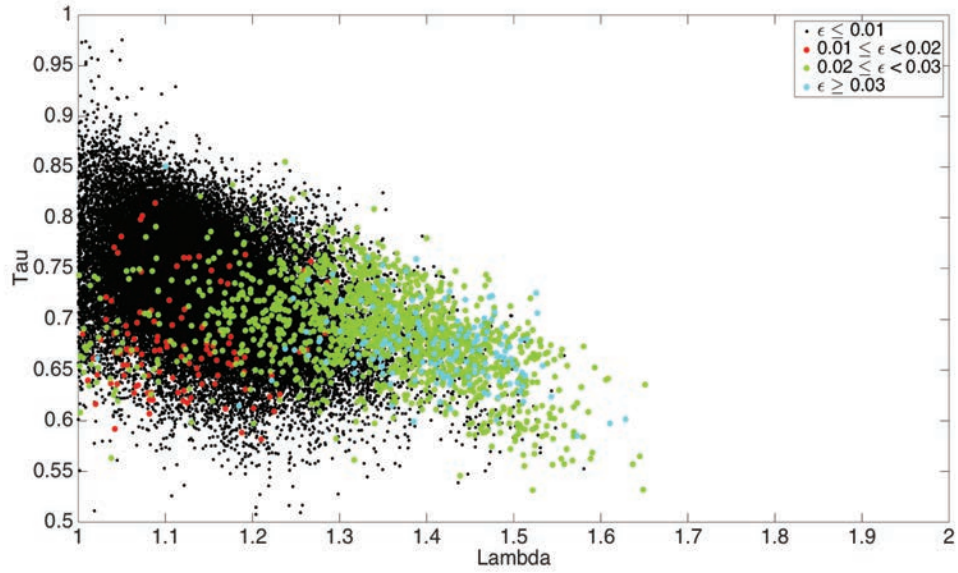

B

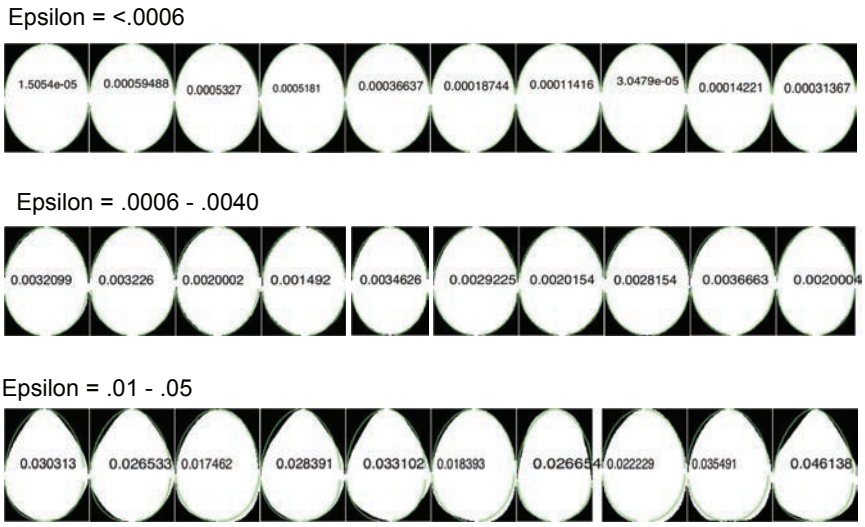

Figure S3. The theoretical morphospace, modified from Baker (*11*), with asymmetry and ellipticity ranging from 0 to 1. Missing from the occupied morphospace (gray points, identical to Fig. 1) are spherical, asymmetric eggs, somewhat similar in shape to a hot air balloon. Hot air balloon image is from Wikimedia Commons and covered by a GNU Free Documentation License.

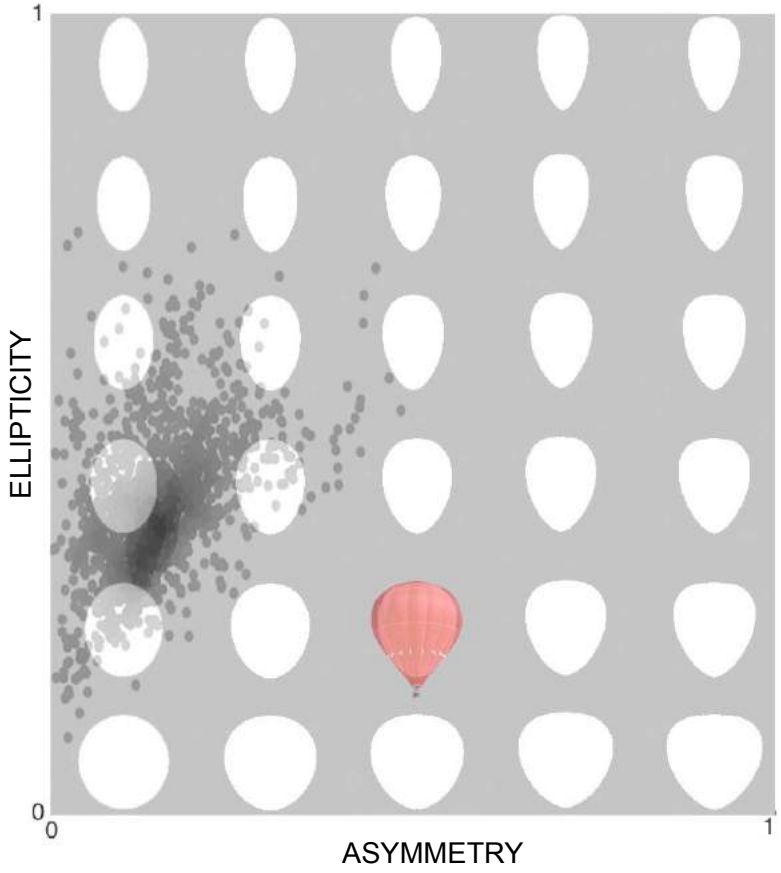

Figure S4. A density map of the egg shape morphospace. The region of shape morphospace containing the most eggs is shown in red **(A)** and in dark blue **(B)**. Frequency histograms are plotted on the x-axis (asymmetry) and the y-axis (ellipticity) in **(B)**.

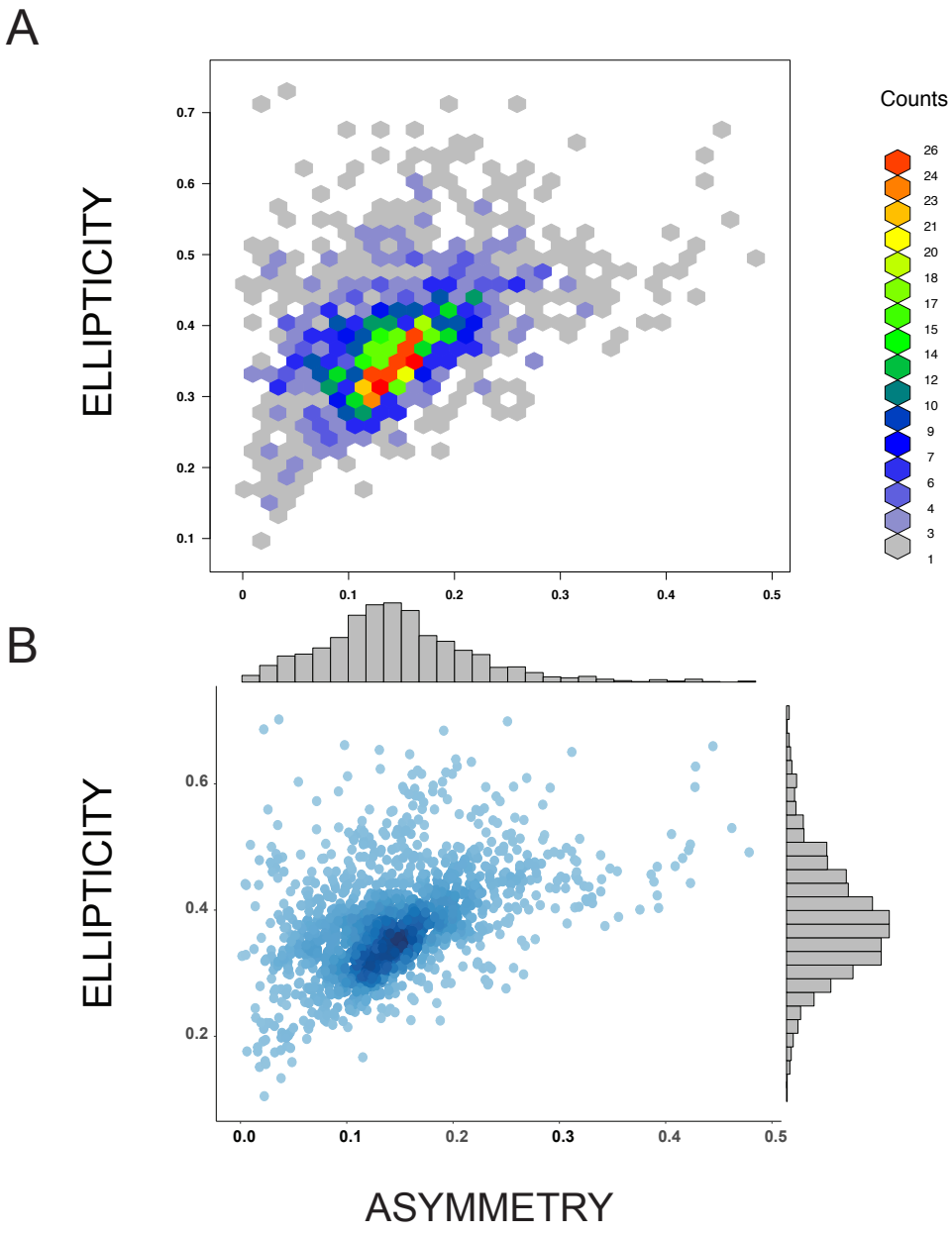

Figure S5. In the literature, there are several suggestions that eggs can be classified into discrete egg shape classes. Our data reveal that these distinctions do not exist, and that the gaps between these presumed egg shape classes, which are modified from (*33*) and shown as light yellow egg shape profiles, are instead filled. Note that none of the presumed egg shapes overlaps the most commonly represented natural egg shape (shown as the red egg shape profile), which falls in the region occupied by the seven red hexagons.

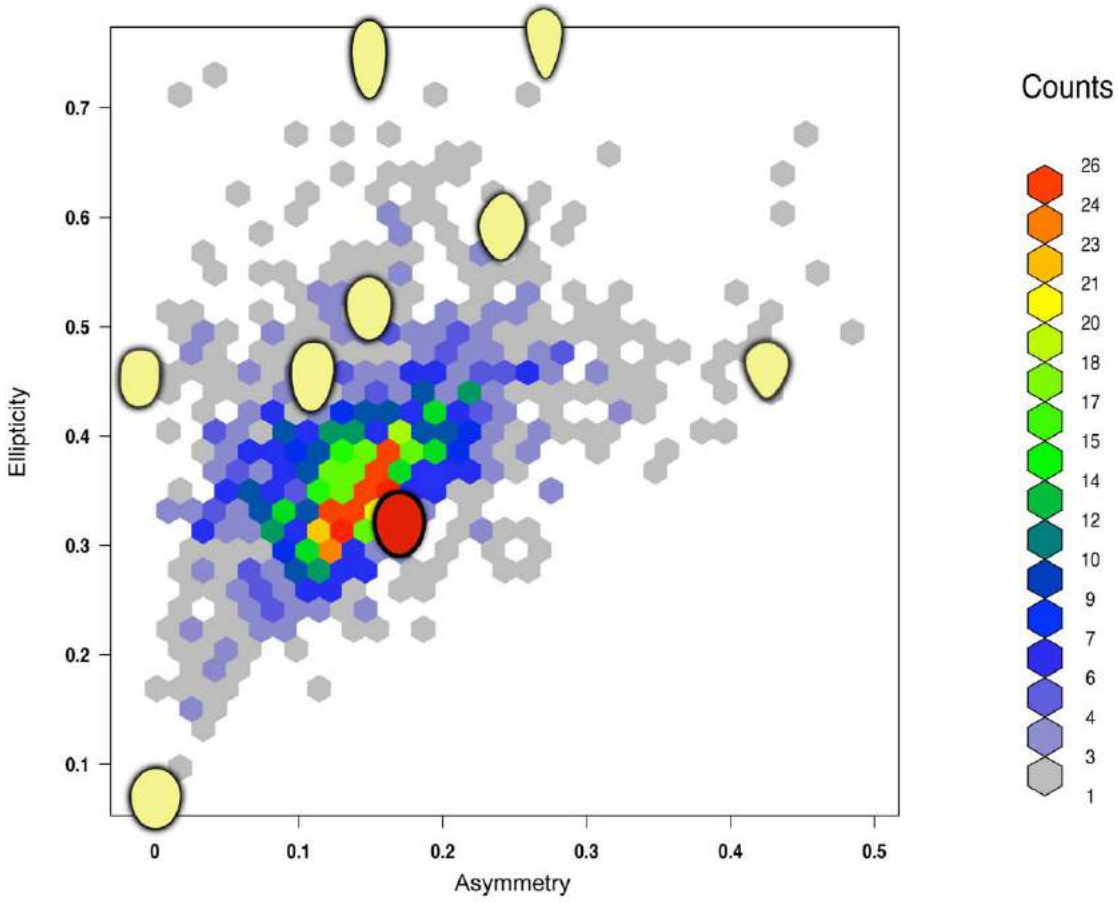

Figure S6. Egg size-shape morphospace (asymmetry versus ellipticity versus major axis length in centimeters) by avian order. Data are the same as those presented in Fig. S4, but here with the major axis length of the egg shown on the z-axis. In addition, extinct species have been omitted.

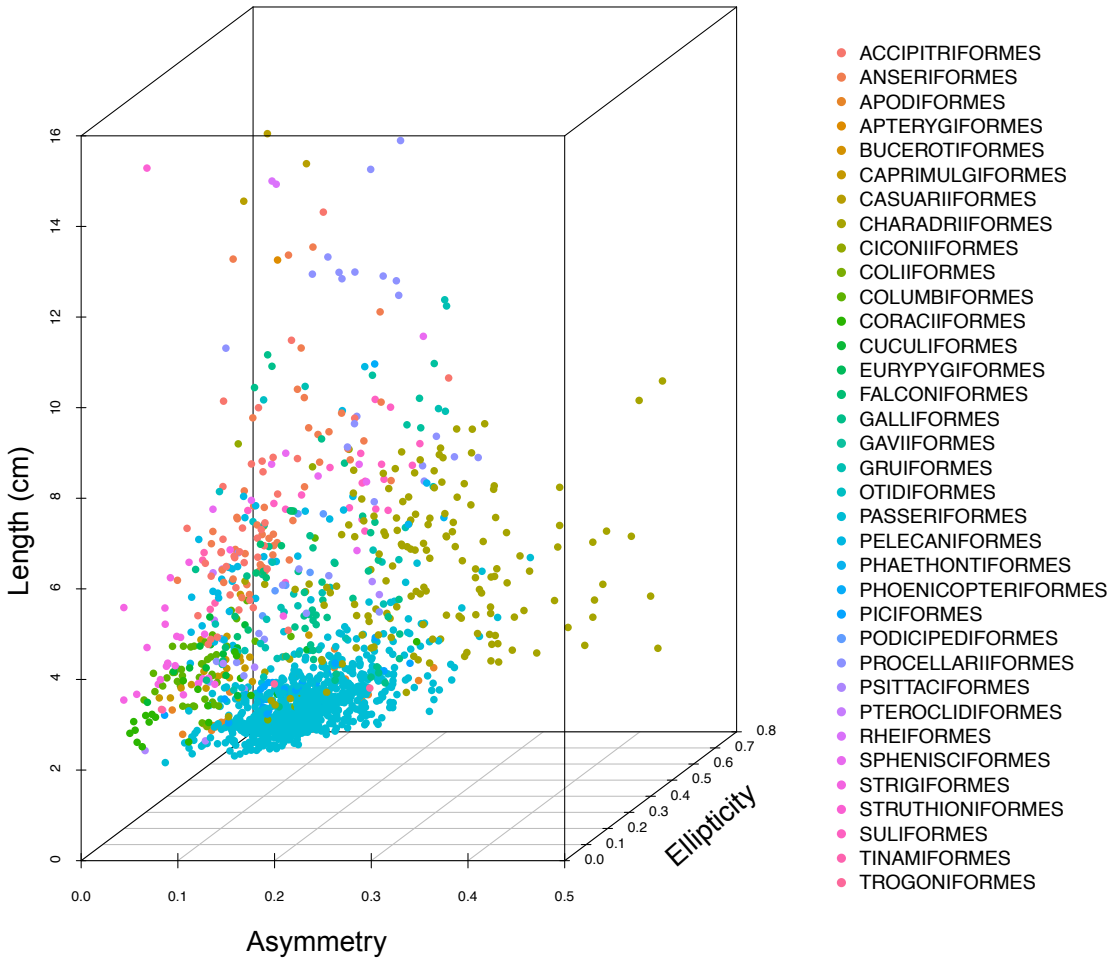

Figure S7. Proportional occupancy of the asymmetry-ellipticity morphospace by different avian orders.

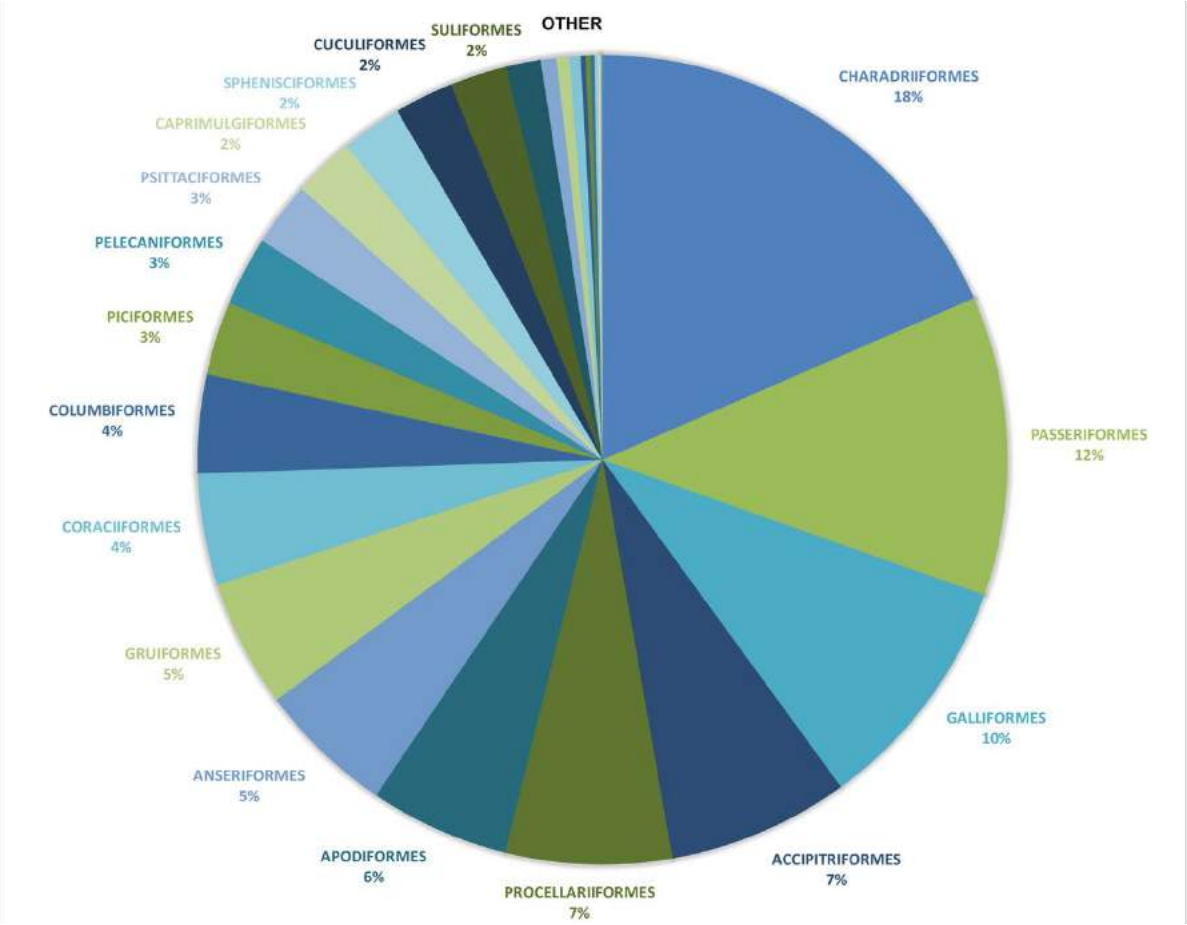

Figure S8. (A) The theoretical morphospace (with asymmetry and ellipticity ranging from 0 to 1), filled with 49,175 individual eggs from our dataset (black dots) and the ~250 eggs in Baker's original paper (*11*) (red dots). **B)** The theoretical morphospace, filled with 49,175 individual eggs from our dataset (black dots) and eggs (including many dinosaurs and non-avian reptiles) from other datasets. The round colored dots represent eggs described in (*16*) converted to our shape morphospace. The triangular colored markers represent eggs described in (*15*), also converted to our shape morphospace.

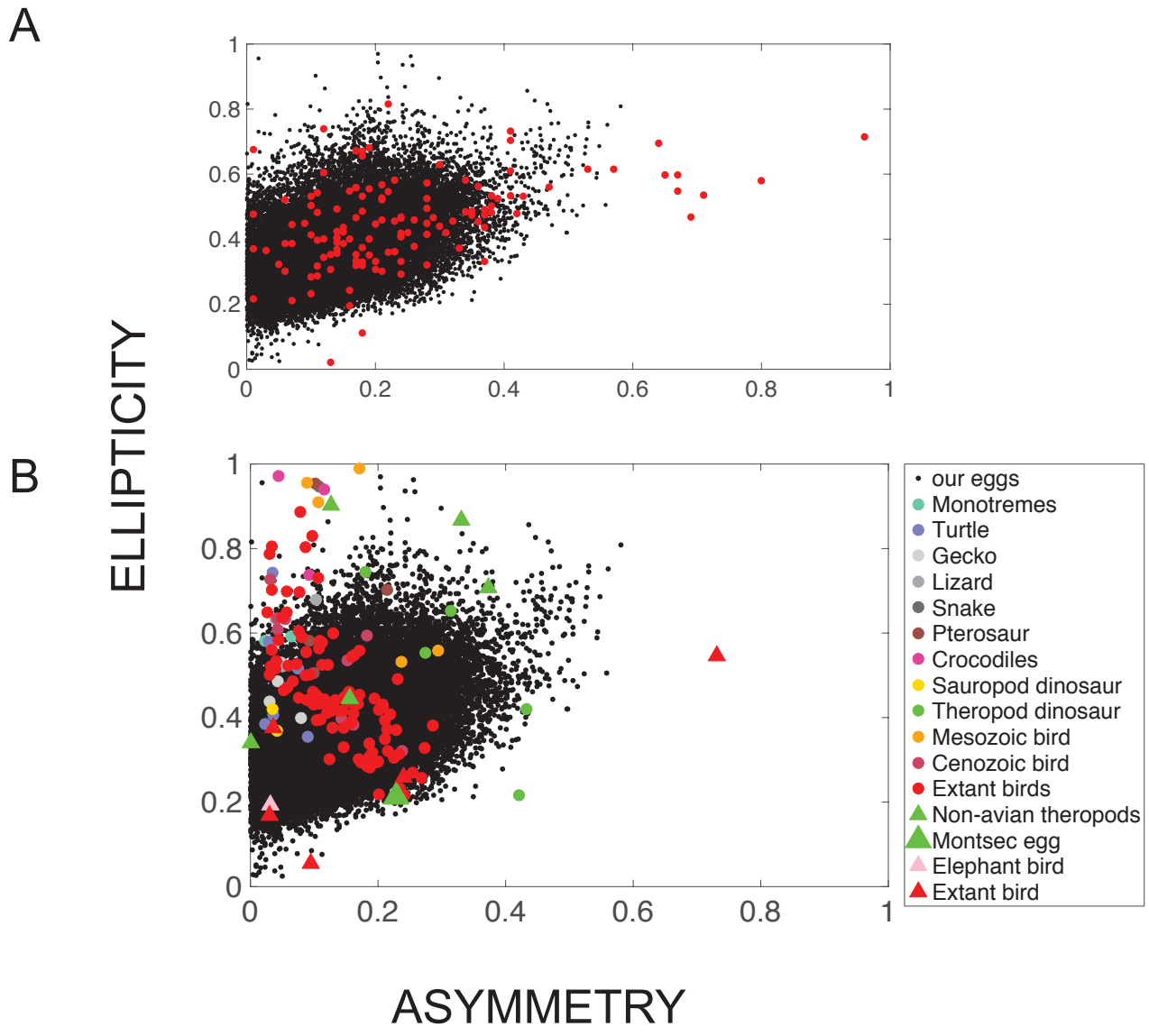

Figure S9. (A,B,C) A simulation showing how an initial circular membrane (black) with uniform properties grows under uniform pressure into an enlarged circular membrane (red). The amount of extension between adjacent pairs of nodes is equal as expected. The extensional stretch ratio is equal as expected. Note that $s = 0$ (A, C, D, F) corresponds to the far right (pointy) end of the egg (see Fig. 3A). **(D,E,F)** A simulation showing how an initial circular membrane (black) with a varying thickness (that leads to a scaled pressure $p(\sigma)$ that we assume has a power law form, resulting in a higher scaled pressure at the pointy end of the egg) grows into an asymmetric egg (red). The extensional stretch ratio in this case is higher at the pointy end where the scaled pressure is higher. The extensional stretch ratio for the pairs of nodes is almost uniform except near the pointy end of egg, where there is significant stretching.

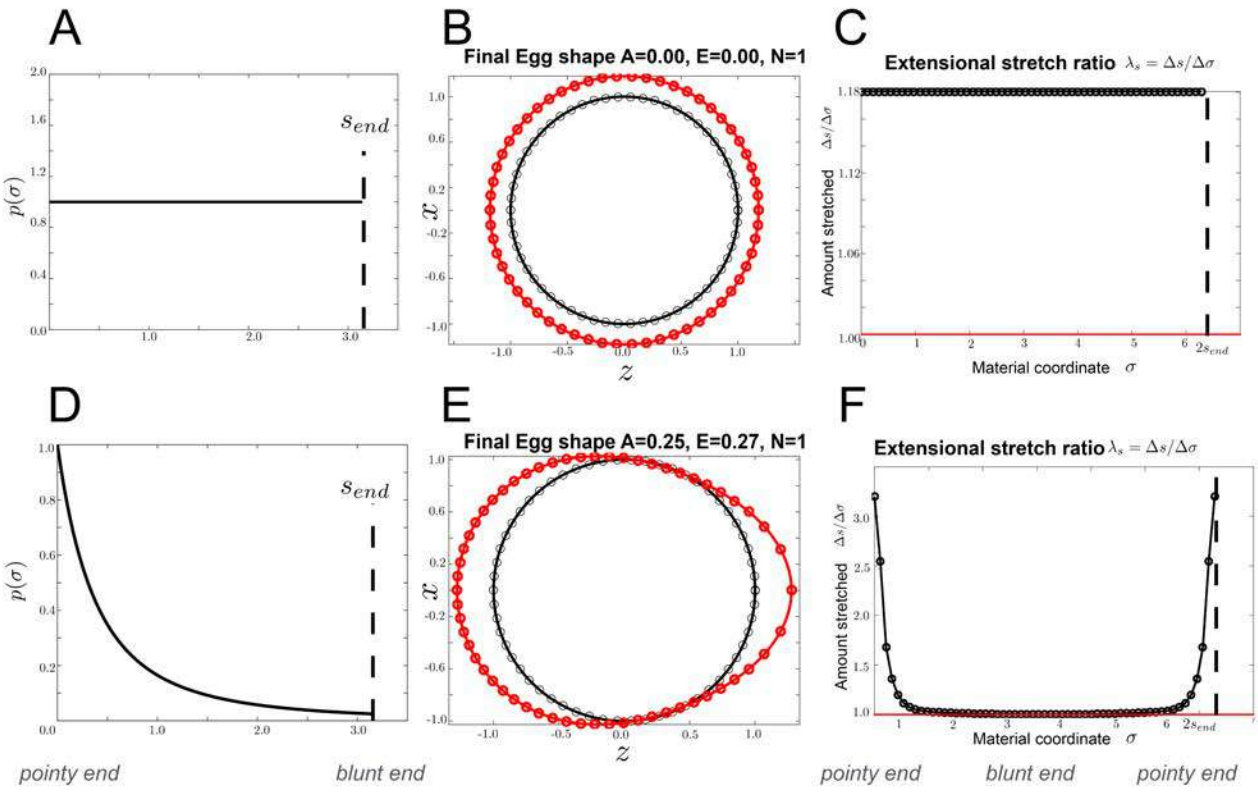

Figure S10. (A,B) An example of a counterfactual egg with A = 0.41 and E = 0.28, obtained using a piecewise varying $A(\sigma), B(\sigma)$. For this egg, $p(\sigma) = (\sigma + a)^{-b}$, $\mu(\sigma) = c + d \tanh[e(\sigma - f)]$ for different growth steps. These functional forms are similar to the equations we used previously, but here we allow $\mu(\sigma)$ to vary smoothly from $(c - d)$ to $(c + d)$ as we move from the pointy end to the blunt end. For this egg, $p(\sigma) = (\sigma + 0.4)^{-2.8}$, $\mu(\sigma) = 0.6 + 0.35 \tanh[1(\sigma - L_0/6)]$, where L_0 is the total longitudinal length of the unstretched membrane. Such counterfactual eggs are not found in nature. In addition, the Baker model (red curve) does not fit this egg (black curve) very well due to the discontinuous nature of the variation of the curve of revolution. **(C,D)** Another example of a counterfactual egg, with A = 1.05 and E = 0.72, is obtained by having a very thin membrane close to a pole, leading to an lemon-like shape. For this egg, $p(\sigma) = (\sigma + 0.5)^{-2.4}$, $\mu(\sigma) = 0.6 + 0.35 \tanh[1(\sigma - L_0/6)]$. The membrane is uniformly thick elsewhere, except at the pointy end; this is similar to having a balloon with a weak spot. The Baker model (red curve) does not fit the egg (black curve) very well due to the presence of an inflection point in the curve.

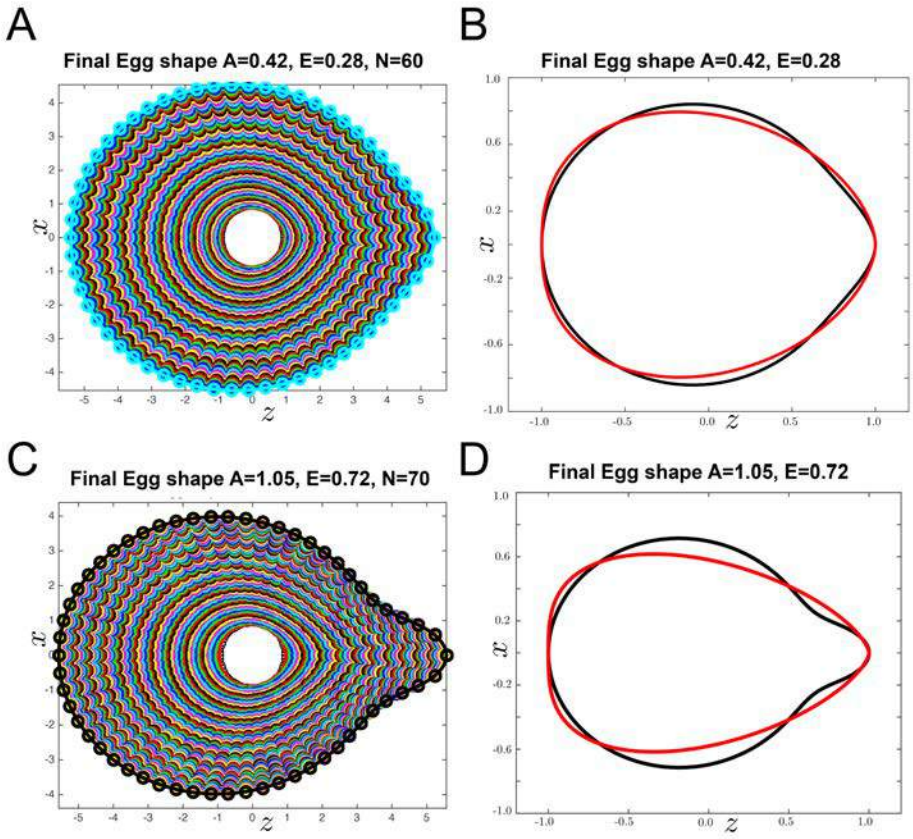

Figure S11. The egg shape morphospace (asymmetry versus ellipticity) for clutches of size 1 to 10. Average clutch size is based on data from (*42*) and from the online Handbook of the Birds of the World Alive (*43*). For example, each species in our dataset with an average clutch size of 1 is represented in the morphospace in the first panel, plotted as a function of the average egg asymmetry and ellipticity for that species. The red dot represents the shape of the optimal (theoretical) egg predicted by Barta and Szekely (*5*).

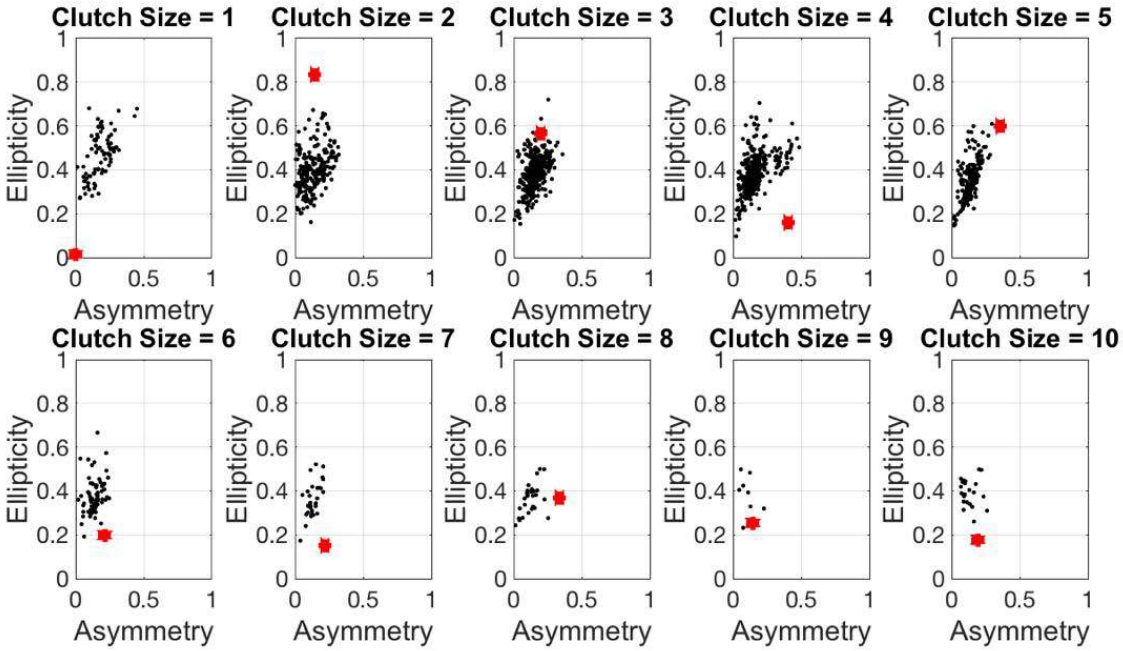

Figure S12. The egg size-shape morphospace (asymmetry versus ellipticity versus length) color-coded by average clutch size. Average clutch size is based on data from (*42*) and from the online Handbook of the Birds of the World Alive (*43*). Species do not converge on exactly the same egg shape if they share the same clutch size.

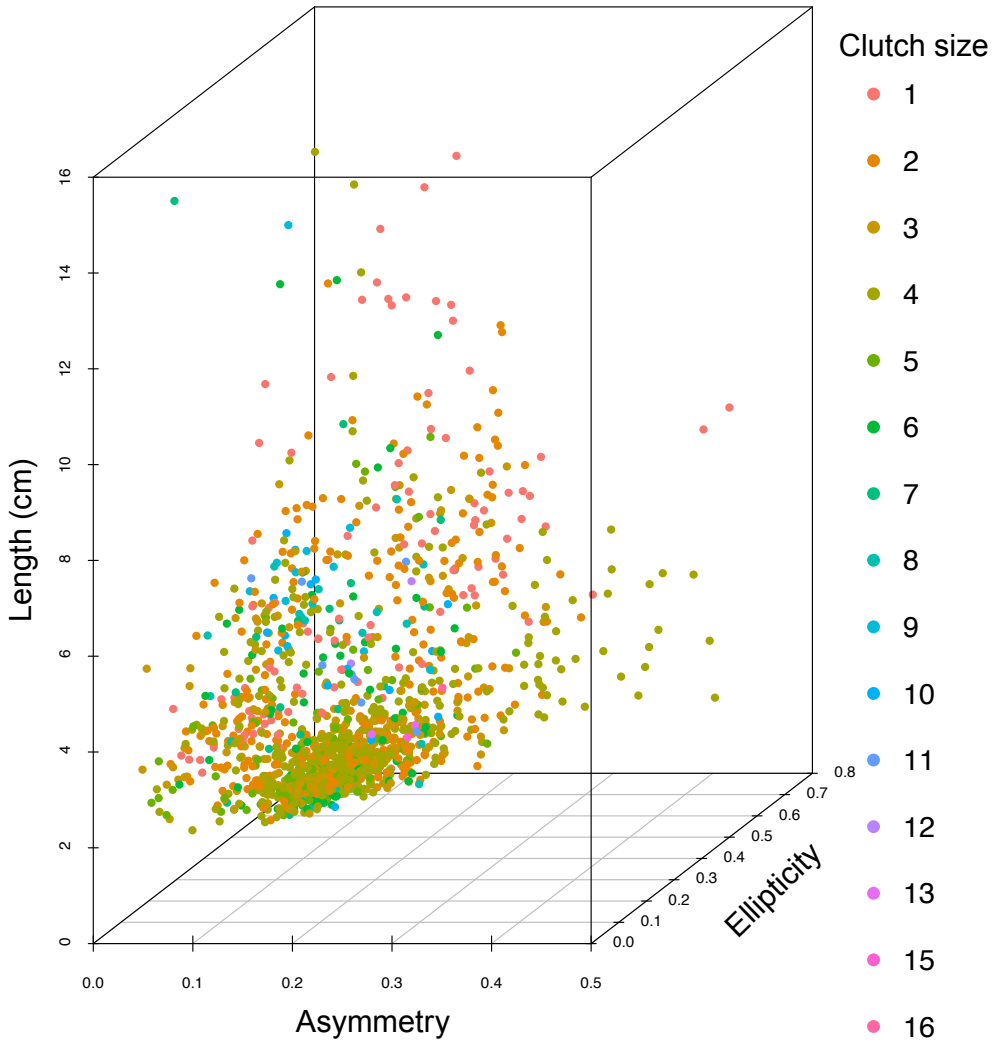

Figure S13. Egg shape is different for flightless penguins vs. flightless ratites. Here we plot the egg shapes for 19 flightless birds in our dataset, including kiwi, ostrich, several species of penguin and a rail. Penguins tend to have more asymmetric eggs, perhaps because their bodies have been streamlined for swimming underwater.

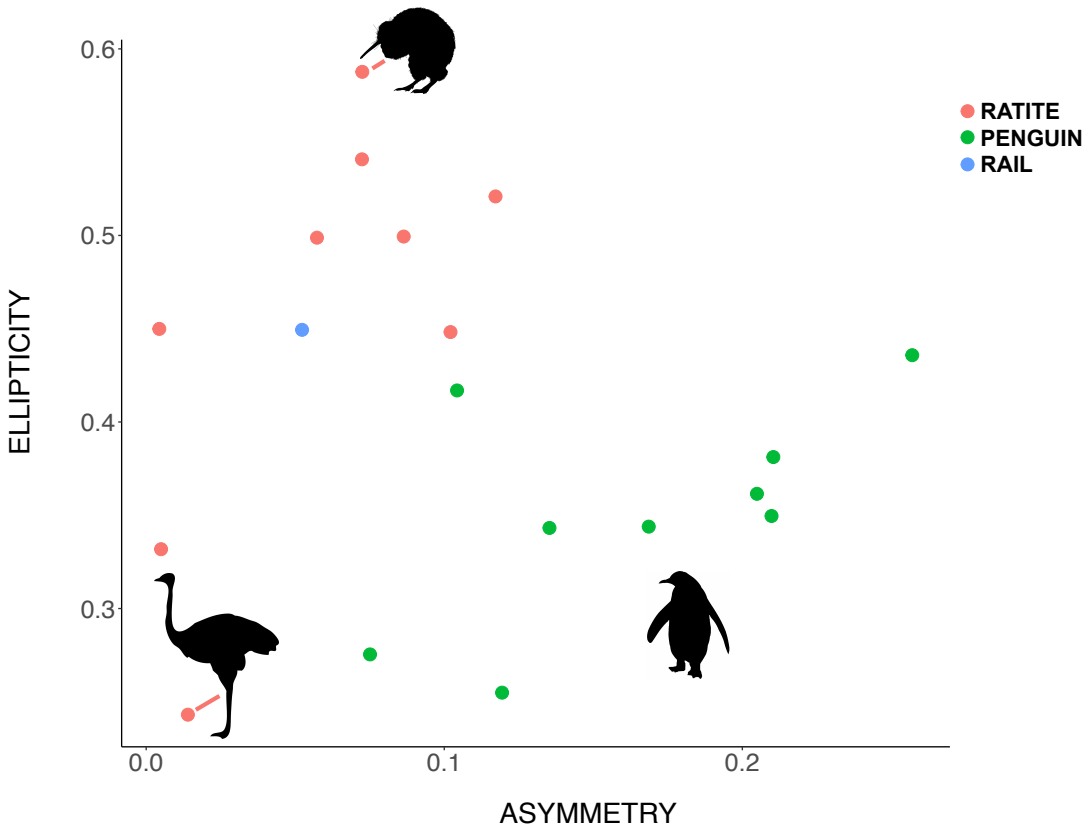

Figure S14. The relationship between flight ability and egg shape. Comparison of egg asymmetry **(A)** and ellipticity **(B)** of birds in the 12 most speciose orders in our sample, based on HWI. We divided species in each order into two groups: low HWI (lower 50%) and high HWI (higher 50%). In general, species with high HWI tend to be more asymmetric (11 of 12 orders) and elliptical (9 of 12 orders) than species with low HWI within the same order. There are exceptions: within Charadriiformes **(C)**, there is not a clear relationship between asymmetry, ellipticity and HWI (lower HWI = red; higher HWI = turquoise). Within Apodiformes **(D)**, in contrast, birds with higher HWI (turquoise, mostly swifts) have more asymmetric eggs than birds with lower HWI (red, mostly hummingbirds). Compared to all birds, both swifts and hummingbirds have very high HWI. It is notable, then, that even within Apodiformes we see a trend toward increased asymmetry with increased HWI.

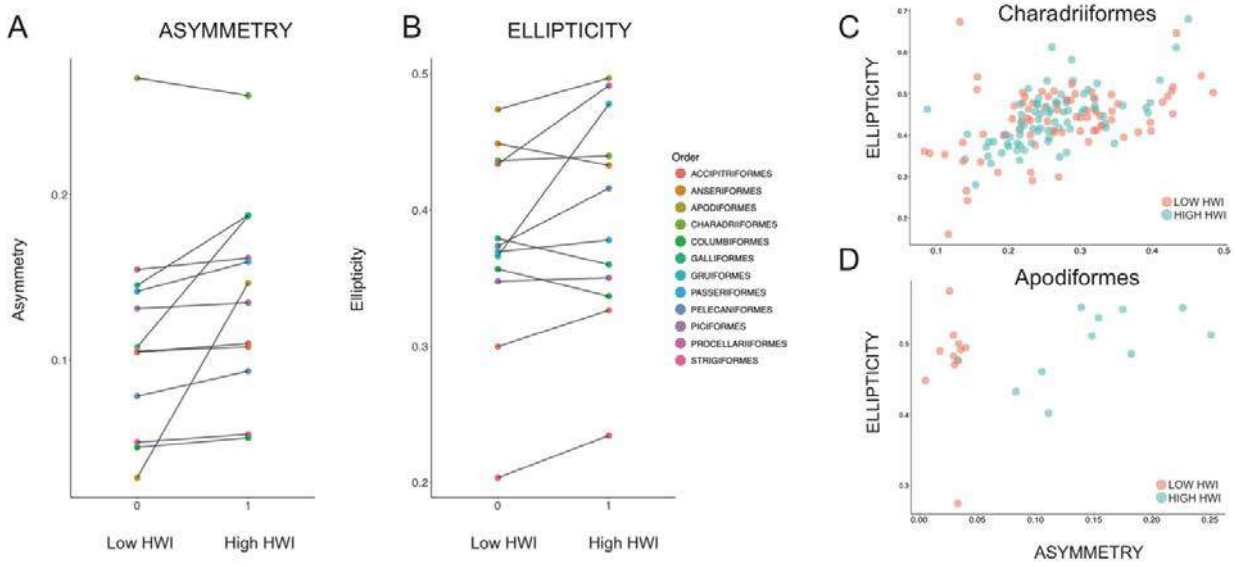

Figure S15. (A) Within Charadriiformes, more precocial birds hatch from more asymmetric eggs (shown here and supported by the comparative analysis). There is a clear relationship between developmental mode and egg asymmetry in this clade. Chick developmental mode was scored in four categories (precocial 1, precocial 2, precocial 3, semiprecocial) following (*54*), where precocial 1 is the most precocial and semiprecocial is the least precocial of these categories. **(B)** Differences in egg asymmetry and ellipticity as a function of developmental mode across all birds. Despite differences, development is not a significant predictor of egg shape across all birds in our sample when we control for phylogenetic relatedness and other fixed effects. Chick developmental mode was scored in eight categories 1-8 (superprecocial, precocial 1, precocial 2, precocial 3, semiprecocial, semialtricial, altricial 1, altricial 2) following (*54*).

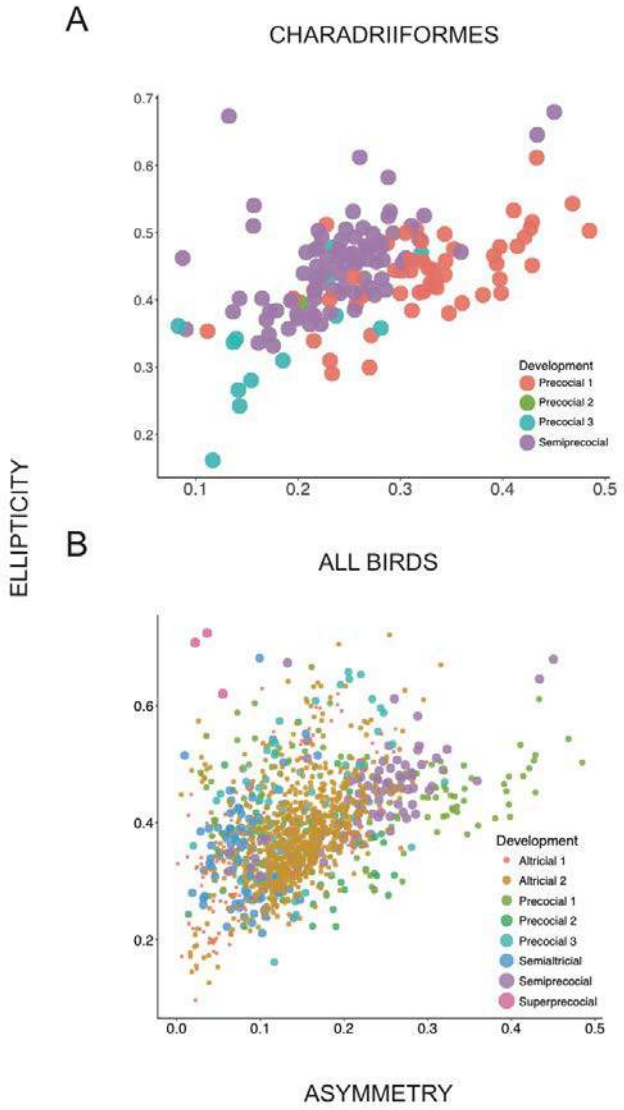

Figure S16. There is a cubic relationship between average egg length (cm) and estimated egg volume (cm^3). There is a linear relationship between the log of average egg length (cm) and the log of estimated egg volume (cm^3). Egg length measurements were taken directly from digital images. Egg volume was estimated from Baker (*11*) using length and the shape parameters. For clarity, eggs with very high volumes (the top 5% in our dataset) are omitted from the graphs below.

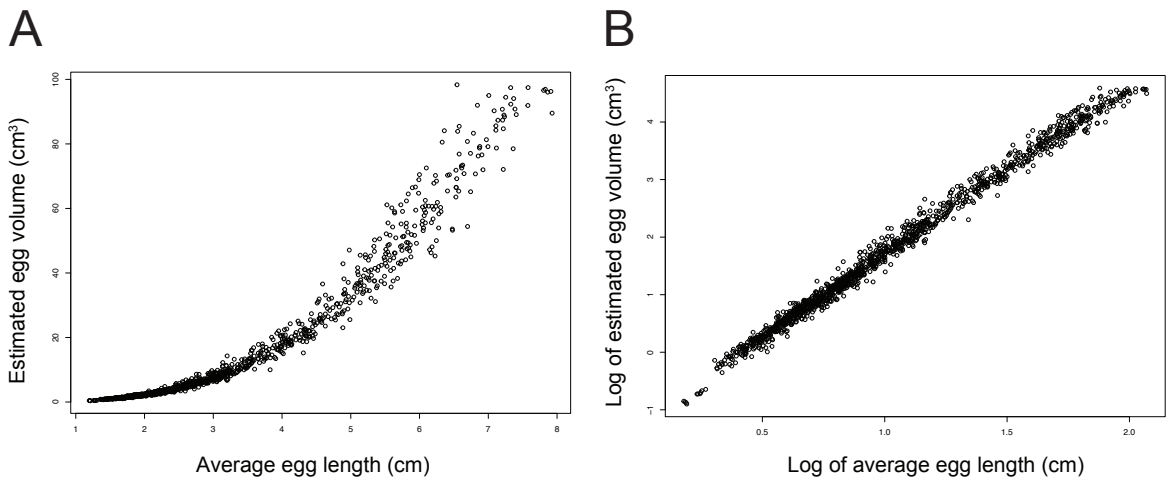

Table S1. Asymmetry-ellipticity morphospace occupancy by different avian orders.

Order	Sample size (number of species)	Morphospace occupancy
Charadriiformes	154	0.1340
Passeriformes	740	0.0868
Galliformes	48	0.0694
Accipitriformes	41	0.0527
Procellariiformes	33	0.0481
Apodiformes	22	0.0405
Anseriformes	48	0.0395
Gruiformes	35	0.0370
Coraciiformes	19	0.0324
Columbiformes	44	0.0286
Piciformes	30	0.0212
Pelecaniformes	31	0.0202
Psittaciformes	6	0.0186
Caprimulgiformes	20	0.0177
Sphenisciformes	9	0.0176
Cuculiformes	14	0.0171
Suliformes	20	0.0164
Strigiformes	24	0.0101
Coliiformes	4	0.0046
Podicipediformes	8	0.0036
Falconiformes	11	0.0033
Trogoniformes	3	0.0014
Ciconiiformes	4	0.0013
Otidiformes	3	0.0012
Casuariiformes	3	0.0011
Gaviiformes	5	0.0004
Phaethontiformes	3	0.0004
Tinamiformes	4	0.0003
Pteroclidiformes	3	0.0001
Rheiformes	2	
Bucerotiformes	1	
Eurypygiformes	1	
Apterygiformes	1	
Phoenicopteriformes	1	
Struthioniformes	1	
Extinct	4	

Table S2-A. PREDICTORS OF EGG LENGTH: ALL BIRDS. Birds lay longer eggs, on average, if they have low clutch size, large body mass, a higher-calcium diet and/or are more precocial. These correlations are significant after controlling for phylogenetic relationships and other fixed effects, and are consistent under different phylogenetic topologies (Prum Tree or Jetz Tree, with Prum tree shown here).

	Bayesian phylogenetic mixed model (BPMM)					
	z	2.5% CL	97.5% CL			
Fixed effects (standardized)				% change	SD	p-value estimate
Intercept	0.023	-0.196	0.258	-	-	0.832
Clutch Size	-0.129	-0.210	-0.062	-8.6	0.038	< 0.001
Nest - Plate	-0.044	-0.246	0.121	-2.9	0.093	0.626
Nest - Cup	-0.029	-0.309	0.193	-1.9	0.128	0.822
Nest - Elevated	-0.031	-0.236	0.175	-2.0	0.106	0.768
Nest - Cavity	-0.035	-0.316	0.198	-2.3	0.130	0.808
HWI	0.039	-0.040	0.122	2.6	0.043	0.392
Body Mass	0.856	0.773	0.941	57.4	0.042	0.001
Latitude	0.060	-0.107	0.240	4.1	0.087	0.454
Temperature	0.017	-0.139	0.205	1.1	0.086	0.864
Precipitation	0.009	-0.064	0.084	0.6	0.037	0.796
Diet	0.064	0.007	0.130	4.3	0.032	0.042
Constrained	0.037	-0.228	0.334	2.5	0.147	0.820
Development	-0.138	-0.249	-0.039	-9.3	0.053	0.010
Random effects				σ^2 %		
Phylogeny (n = 1209)	0.003	0.000	0.011	0.2	-	-
Summary statistics						
DIC	2282.9	-	-	-	-	-
R^2	0.427	-	-	-	-	-

Clutch size: average clutch size per species, obtained from (*42*) and from the online Handbook of the Birds of the World Alive (*43*). **Nest – Plate** and **Nest – Cup:** all nests were scored as one of three shape categories (cup, plate, or scrape), following descriptive information in Handbook of the Birds of the World Alive (*43*); coefficients refer to the amount that the respective variable differs from the reference variable (scrape). **Nest – Elevated** and **Nest – Cavity:** all nests were additionally scored as one of three location categories (cavity, elevated, or non-cavity ground), following descriptive information in Handbook of the Birds of the World Alive (*43*); coefficients refer to the amount that the respective variable differs from the reference variable (non-cavity ground). **HWI:** average adult hand-wing index; **Body mass:** average adult body masses obtained from (*55*) and log-transformed. **Latitude, temperature** and **precipitation:** species-level range median latitude along with mean temperature and precipitation from the Worldclim database (*56*) were calculated from global range polygons (BirdLife International 2011, *Bird species distribution maps of the world*). **Diet:** dietary content, obtained from (*44*), was categorized as herbivorous, mixture of plant and animal diets or carnivorous; coefficients refer to the amount that the respective variable differs

from the reference variable (herbivorous). **Constrained:** binary variable describing whether (1) or not (0) a nest is constrained (a cavity or cup nest). **Development:** Chick developmental mode was scored in eight categories 1-8 (superprecocial, precocial 1, precocial 2, precocial 3, semiprecocial, semialtricial, altricial 1, altricial 2) following (*54*).

In subsequent tables: **PC1:** we performed PCA on egg length and adult body mass; PC1 is the first principal component axis; high values represent long (large) eggs/large adult body mass; **PC2:** we performed PCA on egg length and adult body mass; PC2 is the second principal component axis; PC2 measures whether the egg is longer (positive PC2) or shorter (negative PC2) than expected given the bird's adult body mass.

Table S2-B. PREDICTORS OF EGG ASYMMETRY: ALL BIRDS. Birds lay more asymmetrical eggs, on average, if they have high hand-wing indices and/or large adult body mass/long eggs (PC1). These correlations are significant after controlling for phylogenetic relationships and other fixed effects, and are consistent under different phylogenetic topologies (Prum Tree or Jetz Tree, with Prum Tree results shown here).

	Bayesian phylogenetic mixed model (BPMM)					
	z	2.5% CL	97.5% CL			
Fixed effects (standardized)				% change	SD	p-value estimate
Intercept	-1.105	-1.784	-0.463	-	-	0.002
Clutch Size	-0.022	-0.128	0.077	-1.1	0.053	0.650
Nest - Plate	0.028	-0.201	0.245	1.3	0.114	0.824
Nest - Cup	0.040	-0.292	0.474	1.9	0.191	0.864
Nest - Elevated	-0.117	-0.376	0.146	-5.6	0.137	0.388
Nest - Cavity	-0.224	-0.565	0.116	-10.7	0.177	0.202
HWI	0.155	0.043	0.268	7.4	0.058	0.006
PC1	0.373	0.222	0.514	17.9	0.075	< 0.001
Latitude	-0.061	-0.247	0.127	-2.9	0.096	0.518
Temperature	-0.150	-0.342	0.028	-7.2	0.093	0.096
Precipitation	0.032	-0.044	0.119	1.5	0.041	0.434
Diet	0.008	-0.077	0.097	0.4	0.045	0.890
Constrained	0.223	-0.173	0.598	10.7	0.201	0.268
Development	-0.177	-0.374	0.020	-8.5	0.101	0.070
PC2	0.065	-0.026	0.157	3.1	0.048	0.188
Random effects				σ^2 %		
Phylogeny (n = 1209)	0.412	0.284	0.554	19.7	-	-
Summary statistics						
DIC	2768.9	-	-	-	-	-
R^2	0.511	-	-	-	-	-

Table S2-C. PREDICTORS OF EGG ELLIPTICITY: ALL BIRDS. Birds lay more elliptical eggs, on average, if they have high hand-wing indices, large body mass/long eggs (PC1), longer eggs than expected for their body size (PC2), and/or a diet low in calcium. These correlations are significant after controlling for phylogenetic relationships and other fixed effects, and are consistent under different phylogenetic topologies (Prum Tree or Jetz Tree, with Prum Tree results shown here).

	Bayesian phylogenetic mixed model (BPMM)					
	z	2.5% CL	97.5% CL			
Fixed effects (standardized)				% change	SD	p-value estimate
Intercept	-0.802	-1.425	-0.213	-	-	0.004
Clutch Size	-0.047	-0.146	0.064	-1.6	0.053	0.370
Plate/Cup - Plate	0.202	-0.035	0.435	6.7	0.122	0.102
Plate/Cup - Cup	0.312	-0.074	0.677	10.3	0.192	0.102
Cavity - Elevated	0.087	-0.170	0.341	2.9	0.135	0.518
Cavity - Cavity	0.165	-0.129	0.514	5.5	0.167	0.328
HWI	0.205	0.081	0.315	6.8	0.060	< 0.001
PC1	0.830	0.692	0.986	27.4	0.077	< 0.001
Latitude	-0.068	-0.249	0.117	-2.3	0.095	0.484
Temperature	-0.079	-0.262	0.095	-2.6	0.092	0.390
Precipitation	-0.016	-0.090	0.066	-0.5	0.040	0.708
Diet	-0.090	-0.174	-0.003	-3.0	0.044	0.050
Constrained	-0.167	-0.521	0.209	-5.5	0.188	0.368
Development	0.030	-0.161	0.227	1.0	0.101	0.752
PC2	0.334	0.250	0.434	11.1	0.047	0.001
Random effects				σ^2 %		
Phylogeny (n = 1209)	0.392	0.270	0.537	13.0	-	-
Summary statistics						
DIC	2795.2	-	-	-	-	-
R^2	0.602	-	-	-	-	-

Table S3-A. PREDICTORS OF EGG LENGTH: SEABIRDS. Seabirds lay longer eggs, on average, if they have high body masses. These correlations are significant after controlling for phylogenetic relationships and other fixed effects, and are consistent under different phylogenetic topologies (Prum Tree or Jetz Tree, with Prum Tree results shown here).

	Bayesian phylogenetic mixed model (BPMM)					
	z	2.5% CL	97.5% CL			
Fixed effects (standardized)				% change	SD	p-value estimate
Intercept	-0.166	-0.713	0.352	-	-	0.574
Clutch Size	-0.171	-0.462	0.120	-6.7	0.152	0.264
Nest - Plate	0.002	-0.639	0.565	0.1	0.312	0.990
Nest - Elevated	0.163	-0.467	0.865	6.4	0.350	0.656
Nest - Cavity	0.318	-0.408	1.123	12.5	0.391	0.416
HWI	0.211	-0.104	0.511	8.3	0.161	0.212
Body Mass	1.231	0.865	1.647	48.3	0.198	< 0.001
Latitude	0.053	-0.569	0.756	2.1	0.343	0.886
Temperature	0.057	-0.537	0.756	2.3	0.330	0.906
Precipitation	-0.010	-0.289	0.215	-0.4	0.131	0.918
Diet	-0.008	-0.205	0.227	-0.3	0.113	0.918
Development	-0.257	-0.657	0.177	-10.1	0.218	0.234
Random effects				σ^2 %		
Phylogeny (n = 81)	0.065	0.000	0.222	2.5	-	-
Summary statistics						
DIC	181.8	-	-	-	-	-
R^2	0.560	-	-	-	-	-

Table S3-B. PREDICTORS OF EGG ASYMMETRY: SEABIRDS. Seabirds lay more asymmetric eggs, on average, if they have large body mass/long eggs (PC1). This correlation is significant after controlling for phylogenetic relationships and other fixed effects, and is consistent under different phylogenetic topologies (Prum Tree or Jetz Tree, with Prum Tree results shown here).

	Bayesian phylogenetic mixed model (BPMM)					
	z	2.5% CL	97.5% CL			
Fixed effects (standardized)				% change	SD	p-value estimate
Intercept	0.041	-0.702	0.782	-	-	0.894
Clutch Size	-0.021	-0.434	0.332	-0.8	0.193	0.898
Nest - Plate	-0.368	-1.005	0.325	-13.8	0.338	0.266
Nest - Elevated	0.229	-0.508	0.910	8.6	0.377	0.538
Nest - Cavity	-0.141	-0.958	0.708	-5.3	0.418	0.746
HWI	0.310	-0.076	0.724	11.6	0.202	0.102
PC1	0.564	0.162	0.923	21.2	0.200	0.010
Latitude	0.126	-0.642	0.772	4.7	0.361	0.742
Temperature	0.006	-0.740	0.639	0.2	0.353	0.988
Precipitation	-0.055	-0.307	0.208	-2.1	0.135	0.676
Diet	0.014	-0.206	0.258	0.5	0.120	0.906
Development	-0.345	-0.959	0.366	-13.0	0.338	0.298
PC2	-0.133	-0.543	0.361	-5.0	0.233	0.566
Random effects				σ^2 %		
Phylogeny (n = 81)	0.350	0.000	0.915	13.1	-	-
Summary statistics						
DIC	217.1	-	-	-	-	-
R^2	0.571	-	-	-	-	-

Table S3-C. PREDICTORS OF EGG ELLIPTICITY: SEABIRDS. Seabirds lay more elliptical eggs, on average, if they have large adult body mass/long eggs (PC1), elevated nests, and/or longer eggs for their size (PC2). These correlations are significant after controlling for phylogenetic relationships and other fixed effects, and are consistent under different phylogenetic topologies (Prum Tree or Jetz Tree, with Prum Tree results shown here).

	Bayesian phylogenetic mixed model (BPMM)					
	z	2.5% CL	97.5% CL			
Fixed effects (standardized)				% change	SD	p-value estimate
Intercept	-0.389	-1.070	0.213	-	-	0.226
Clutch Size	0.315	-0.023	0.706	8.0	0.186	0.084
Nest - Plate	0.186	-0.420	0.824	4.7	0.318	0.544
Nest - Elevated	0.935	0.207	1.653	23.7	0.366	0.010
Nest - Cavity	0.128	-0.732	0.861	3.3	0.407	0.750
HWI	0.184	-0.245	0.545	4.7	0.195	0.322
PC1	0.474	0.087	0.809	12.0	0.186	0.006
Latitude	0.340	-0.330	1.051	8.6	0.351	0.322
Temperature	0.315	-0.367	0.950	8.0	0.340	0.366
Precipitation	0.027	-0.210	0.323	0.7	0.140	0.844
Diet	0.007	-0.226	0.237	0.2	0.117	0.960
Development	0.328	-0.155	0.892	8.3	0.269	0.180
PC2	0.537	0.139	0.989	13.6	0.217	0.010
Random effects				σ^2 %		
Phylogeny (n = 81)	0.161	0.000	0.532	4.1	-	-
Summary statistics						
DIC	201.1	-	-	-	-	-
R^2	0.663	-	-	-	-	-

TABLE S4-A. PREDICTORS OF EGG LENGTH: PASSERIFORMES. Passerines lay longer eggs, on average, if they have high body masses and/or low clutch sizes. These correlations are significant after controlling for phylogenetic relationships and other fixed effects, and are consistent under different phylogenetic topologies (Prum Tree or Jetz Tree, with Prum Tree results shown here).

	Bayesian phylogenetic mixed model (BPMM)					
	z	2.5% CL	97.5% CL			
Fixed effects (standardized)				% change	SD	p-value estimate
Intercept	-0.244	-1.419	0.785	-	-	0.694
Clutch Size	-0.209	-0.314	-0.106	-10.9	0.054	< 0.001
Nest - Plate	0.211	-0.880	1.253	11.0	0.552	0.694
Nest - Cup	0.097	-0.875	1.098	5.1	0.510	0.850
Nest - Elevated	0.055	-0.274	0.410	2.8	0.178	0.792
Nest - Cavity	0.032	-0.391	0.385	1.6	0.201	0.886
HWI	-0.026	-0.122	0.071	-1.4	0.049	0.602
Body Mass	0.900	0.816	0.982	46.9	0.043	< 0.001
Latitude	0.156	-0.080	0.398	8.1	0.123	0.202
Temperature	0.027	-0.185	0.243	1.4	0.110	0.794
Precipitation	0.012	-0.094	0.113	0.6	0.052	0.810
Diet	0.069	-0.009	0.146	3.6	0.041	0.088
Constrained	0.104	-0.401	0.719	5.4	0.285	0.744
Development	-0.017	-0.105	0.063	-0.9	0.043	0.720
Random effects				σ^2 %		
Phylogeny (n = 654)	0.007	0.000	0.023	0.3	-	-
Summary statistics						
DIC	1316.5	-	-	-	-	-
R^2	0.490	-	-	-	-	-

TABLE S4-B. PREDICTORS OF EGG ASYMMETRY: PASSERIFORMES. Passerines lay more asymmetric eggs, on average, if they have high hand-wing indices, large body mass/long eggs (PC1), longer eggs for their body mass (PC2), and/or live in regions with low temperatures and/or high precipitation. These correlations are significant after controlling for phylogenetic relationships and other fixed effects, but when the Jetz Tree is used instead of the Prum Tree, precipitation is no longer a significant predictor. Both phylogenetic topologies are presented here.

Prum Tree

	Bayesian phylogenetic mixed model (BPMM)					
	z	2.5% CL	97.5% CL			
Fixed effects (standardized)				% change	SD	p-value estimate
Intercept	-0.321	-1.588	0.909	-	-	0.620
Clutch Size	-0.058	-0.177	0.062	-2.0	0.060	0.342
Nest - Plate	0.375	-0.779	1.436	13.1	0.583	0.526
Nest - Cup	0.161	-1.042	1.093	5.6	0.537	0.784
Nest - Elevated	-0.001	-0.403	0.320	0.0	0.186	0.988
Nest - Cavity	-0.254	-0.658	0.111	-8.9	0.202	0.218
HWI	0.209	0.107	0.330	7.3	0.056	< 0.001
PC1	0.593	0.445	0.726	20.7	0.073	< 0.001
Latitude	-0.188	-0.437	0.039	-6.6	0.126	0.136
Temperature	-0.244	-0.467	-0.034	-8.5	0.117	0.028
Precipitation	0.105	0.004	0.209	3.7	0.054	0.042
Diet	-0.017	-0.110	0.095	-0.6	0.052	0.758
Constrained	0.215	-0.448	0.773	7.5	0.316	0.482
Development	-0.030	-0.130	0.046	-1.1	0.045	0.512
PC2	0.273	0.155	0.408	9.5	0.067	< 0.001
Random effects				σ^2 %		
Phylogeny (n = 654)	0.143	0.028	0.276	5.0	-	-
Summary statistics						
DIC	1663.6	-	-	-	-	-
R^2	0.589	-	-	-	-	-

Jetz Tree

	Bayesian phylogenetic mixed model (BPMM)					
	z	2.5% CL	97.5% CL			
Fixed effects (standardized)				% change	SD	p-value estimate
Intercept	-0.314	-1.501	1.013	-	-	0.594
Clutch Size	-0.060	-0.183	0.049	-2.1	0.060	0.318
Nest - Plate	0.375	-0.839	1.440	13.1	0.596	0.524
Nest - Cup	0.154	-0.850	1.291	5.4	0.562	0.780
Nest - Elevated	0.002	-0.369	0.366	0.1	0.186	0.962
Nest - Cavity	-0.255	-0.706	0.104	-8.9	0.209	0.246
HWI	0.206	0.098	0.323	7.2	0.057	< 0.001
PC1	0.592	0.451	0.737	20.7	0.074	< 0.001
Latitude	-0.186	-0.432	0.074	-6.5	0.129	0.150
Temperature	-0.248	-0.495	-0.016	-8.7	0.121	0.050
Precipitation	0.107	-0.002	0.209	3.7	0.054	0.052
Diet	-0.012	-0.115	0.079	-0.4	0.051	0.834
Constrained	0.217	-0.324	0.864	7.6	0.307	0.486
Development	-0.032	-0.114	0.074	-1.1	0.046	0.462
PC2	0.274	0.146	0.410	9.6	0.067	< 0.001
Random effects				σ^2 %		
Phylogeny (n = 654)	0.143	0.023	0.267	5.0	-	-
Summary statistics						
DIC	1669.9	-	-	-	-	-
R^2	0.589	-	-	-	-	-

TABLE S4-C. PREDICTORS OF EGG ELLIPTICITY: PASSERIFORMES. Passerines lay more elliptical eggs, on average, if they have high hand-wing indices, large body mass/long eggs (PC1), and/or longer eggs for their body mass (PC2). These correlations are significant after controlling for phylogenetic relationships and other fixed effects, but when the Jetz Tree is used instead of the Prum Tree, small clutch size is also correlated with more elliptical eggs. Both phylogenetic topologies are presented here.

Prum Tree

	Bayesian phylogenetic mixed model (BPMM)					
	z	2.5% CL	97.5% CL			
Fixed effects (standardized)				% change	SD	p-value estimate
Intercept	-0.295	-1.452	0.982	-	-	0.630
Clutch Size	-0.118	-0.232	0.004	-3.6	0.062	0.056
Nest - Plate	0.111	-1.128	1.130	3.4	0.578	0.810
Nest - Cup	-0.015	-1.201	0.902	-0.5	0.542	0.998
Nest - Elevated	0.200	-0.161	0.569	6.1	0.187	0.278
Nest - Cavity	0.405	-0.016	0.805	12.4	0.213	0.052
HWI	0.159	0.054	0.269	4.9	0.056	0.002
PC1	0.884	0.736	1.052	27.1	0.079	< 0.001
Latitude	-0.172	-0.401	0.070	-5.3	0.122	0.158
Temperature	-0.122	-0.356	0.090	-3.7	0.117	0.312
Precipitation	-0.031	-0.133	0.076	-0.9	0.055	0.590
Diet	-0.100	-0.212	-0.002	-3.1	0.054	0.056
Constrained	-0.172	-0.717	0.432	-5.3	0.305	0.560
Development	-0.068	-0.146	0.026	-2.1	0.045	0.120
PC2	0.534	0.394	0.656	16.4	0.069	0.001
Random effects				σ^2 %		
Phylogeny (n = 654)	0.173	0.073	0.293	5.3	-	-
Summary statistics						
DIC	1586.0	-	-	-	-	-
R^2	0.620	-	-	-	-	-

Jetz Tree

	Bayesian phylogenetic mixed model (BPMM)					
	z	2.5% CL	97.5% CL			
Fixed effects (standardized)				% change	SD	p-value estimate
Intercept	-0.299	-1.546	0.929	-	-	0.678
Clutch Size	-0.121	-0.241	-0.005	-3.8	0.062	0.048
Nest - Plate	0.125	-1.010	1.261	3.9	0.603	0.848
Nest - Cup	-0.035	-1.134	1.086	-1.1	0.555	0.932
Nest - Elevated	0.192	-0.154	0.571	6.0	0.186	0.320
Nest - Cavity	0.382	-0.032	0.803	11.8	0.209	0.064
HWI	0.157	0.038	0.265	4.9	0.059	0.014
PC1	0.882	0.732	1.033	27.4	0.078	< 0.001
Latitude	-0.178	-0.424	0.059	-5.5	0.126	0.136
Temperature	-0.135	-0.361	0.106	-4.2	0.119	0.246
Precipitation	-0.019	-0.129	0.086	-0.6	0.056	0.718
Diet	-0.095	-0.195	0.003	-3.0	0.053	0.076
Constrained	-0.128	-0.722	0.521	-4.0	0.313	0.702
Development	-0.068	-0.154	0.025	-2.1	0.045	0.140
PC2	0.535	0.400	0.669	16.6	0.070	< 0.001
Random effects				σ^2 %		
Phylogeny (n = 654)	0.171	0.052	0.297	5.3	-	-
Summary statistics						
DIC	1597.0	-	-	-	-	-
R^2	0.617	-	-	-	-	-

TABLE S5-A. PREDICTORS OF EGG LENGTH: CHARADRIIFORMES.

Charadriiformes lay longer eggs, on average, if they have high hand-wing indices and/or large body mass. These correlations are significant after controlling for phylogenetic relationships and other fixed effects, and are consistent under different phylogenetic topologies (Prum Tree or Jetz Tree, with Prum Tree results shown here).

	Bayesian phylogenetic mixed model (BPMM)					
	z	2.5% CL	97.5% CL			
Fixed effects (standardized)				% change	SD	p-value estimate
Intercept	-0.064	-0.328	0.218	-	-	0.662
Clutch Size	-0.181	-0.502	0.120	-6.8	0.160	0.240
Nest - Plate	0.034	-0.363	0.406	1.3	0.197	0.846
Nest - Cup	0.268	-1.043	1.710	10.1	0.711	0.686
Nest - Elevated	0.223	-0.587	0.977	8.4	0.411	0.566
Nest - Cavity	0.331	-0.422	1.077	12.5	0.391	0.406
HWI	0.239	0.011	0.470	9.0	0.118	0.044
Body Mass	0.921	0.723	1.143	34.7	0.108	< 0.001
Latitude	0.125	-0.392	0.677	4.7	0.281	0.650
Temperature	0.083	-0.414	0.644	3.1	0.273	0.804
Precipitation	-0.012	-0.238	0.166	-0.5	0.102	0.918
Diet	-0.010	-0.196	0.175	-0.4	0.097	0.916
Development	-0.207	-0.534	0.080	-7.8	0.158	0.192
Random effects				σ^2 %		
Phylogeny (n = 139)	0.023	0.000	0.090	0.9	-	-
Summary statistics						
DIC	292.4	-	-	-	-	-
R^2	0.571	-	-	-	-	-

TABLE S5-B. PREDICTORS OF EGG ASYMMETRY: CHARADRIIFORMES.

Charadriiformes lay more asymmetric eggs, on average, if they have large body mass/long eggs (PC1) and/or they are more precocial (with developmental mode scored ordinally from 1 [superprecocial] to 8 [altricial 2]). This correlation is significant after controlling for phylogenetic relationships and other fixed effects, and is consistent under different phylogenetic topologies (Prum Tree or Jetz Tree, with Prum Tree results shown here).

	Bayesian phylogenetic mixed model (BPMM)					
	z	2.5% CL	97.5% CL			
Fixed effects (standardized)				% change	SD	p-value estimate
Intercept	0.083	-0.284	0.473	-	-	0.656
Clutch Size	0.060	-0.257	0.409	1.8	0.176	0.708
Nest - Plate	-0.188	-0.634	0.200	-5.7	0.214	0.380
Nest - Cup	0.643	-0.792	2.018	19.5	0.760	0.406
Nest - Elevated	0.108	-0.755	0.896	3.3	0.429	0.820
Nest - Cavity	-0.563	-1.481	0.229	-17.0	0.427	0.168
HWI	0.220	-0.057	0.480	6.7	0.135	0.094
PC1	0.282	0.041	0.470	8.5	0.111	0.008
Latitude	0.082	-0.456	0.595	2.5	0.278	0.780
Temperature	-0.136	-0.610	0.388	-4.1	0.263	0.594
Precipitation	0.052	-0.138	0.244	1.6	0.098	0.592
Diet	-0.087	-0.300	0.096	-2.6	0.103	0.394
Development	-0.683	-1.067	-0.321	-20.7	0.186	< 0.001
PC2	0.125	-0.112	0.342	3.8	0.119	0.304
Random effects				σ^2 %		
Phylogeny (n = 139)	0.073	0.000	0.262	2.2	-	-
Summary statistics						
DIC	348.5	-	-	-	-	-
R^2	0.623	-	-	-	-	-

TABLE S5-C. PREDICTORS OF EGG ELLIPTICITY: CHARADRIIFORMES.

Charadriiformes lay more elliptical eggs, on average, if they have large body mass/long eggs (PC1) or elevated nests. These correlations are significant after controlling for phylogenetic relationships and other fixed effects, and are consistent under different phylogenetic topologies (Prum Tree or Jetz Tree, with Prum Tree results shown here).

	Bayesian phylogenetic mixed model (BPMM)					
	z	2.5% CL	97.5% CL			
Fixed effects (standardized)				% change	SD	p-value estimate
Intercept	-0.083	-0.512	0.250	-	-	0.594
Clutch Size	0.084	-0.244	0.429	2.5	0.171	0.608
Nest - Plate	-0.060	-0.502	0.336	-1.8	0.214	0.764
Nest - Cup	-0.059	-1.403	1.432	-1.8	0.737	0.940
Nest - Elevated	1.030	0.160	1.827	31.1	0.428	0.028
Nest - Cavity	0.520	-0.258	1.374	15.7	0.428	0.226
HWI	0.228	-0.032	0.513	6.9	0.144	0.112
PC1	0.534	0.312	0.752	16.1	0.114	< 0.001
Latitude	0.069	-0.530	0.607	2.1	0.297	0.792
Temperature	-0.015	-0.558	0.536	-0.5	0.282	0.982
Precipitation	0.137	-0.063	0.333	4.1	0.102	0.180
Diet	0.061	-0.131	0.283	1.9	0.109	0.588
Development	-0.309	-0.704	0.055	-9.3	0.193	0.116
PC2	0.125	-0.069	0.378	3.8	0.114	0.256
Random effects				σ^2 %		
Phylogeny (n = 139)	0.077	0.000	0.301	2.3	-	-
Summary statistics						
DIC	366.9	-	-	-	-	-
R^2	0.623	-	-	-	-	-

REFERENCES:

1. P. M. Sander, Reproduction in Early Amniotes. *Science*. **337**, 806–808 (2012).

2. M. E. Hauber, *The Book of Eggs* (Chicago, IL: University of Chicago Press, 2014).

3. T. Birkhead, *The Most Perfect Thing: Inside (and Outside) a Bird's Egg* (Bloomsbury Publishing USA, 2016).

4. N. G. Smith, Adaptations to Cliff-Nesting in Some Arctic Gulls (Larus). *Ibis*. **108**, 68–83 (1966).

5. Z. Barta, T. Szekely, The optimal shape of avian eggs. *Funct. Ecol.* **11**, 656–662 (1997).

6. J. Hutchinson, Three into two doesn't go: two-dimensional models of bird eggs, snail shells and plant roots. *Biol. J. Linn. Soc.* **70**, 161–187 (2000).

7. A. G. Gosler, J. P. Higham, S. J. Reynolds, Why are birds' eggs speckled? *Ecol. Lett.* **8**, 1105–1113 (2005).

8. I. Smart, *Egg-shape in birds* (Egg Incubation: Its Effects on Embyonic Development in Birds and Reptiles, Cambridge, 1991).

9. T. R. Birkhead, J. E. Thompson, D. Jackson, J. D. Biggins, The point of a Guillemot's egg. *Ibis*. **159**, 255–265 (2017).

10. J. B. Iverson, M. A. Ewert, Physical characteristics of reptilian eggs and a comparison with avian eggs. *Egg Incubation: Its Effect on Embryonic Development in Birds and Reptiles. Cambridge University Press, New York, New York, USA*, 87–100 (1991).

11. D. Baker, A geometric method for determining shape of bird eggs. *Auk*. **119**, 1179–1186 (2002).

12. F. W. Preston, The shapes of birds' eggs. *Auk*. **70**, 160–182 (1953).

13. S. M. Supplement, Materials and methods are available as supplementary materials on *Science* Online.

14. D. K. Zelenitsky, Reproductive traits of non-avian theropods. *J. Paleont. Soc. Korea*. **22**, 209–216 (2006).

15. N. López-Martínez, E. Vicens, A new peculiar dinosaur egg, *Sankofa pyrenaica* oogen. nov. oosp. nov. from the Upper Cretaceous coastal deposits of the Aren Formation, south-central Pyrenees, Lleida, Catalonia, Spain. *Palaeontology*. **55**, 325–339 (2012).

16. D. C. Deeming, M. Ruta, Egg shape changes at the theropod-bird transition, and a morphometric study of amniote eggs. *R. Soc. Open Sci.* **1**, 140311–140311 (2014).

17. J. R. G. Bradfield, Radiographic studies on the formation of the hen's egg shell. *J. Exp. Biol.* **28**, 125–140 (1951).

18. M. T. Hincke *et al.*, The eggshell: structure, composition and mineralization. *Front. Biosci.* **17**, 1266–1280 (2012).

19. K.-M. Mao, F. Sultana, M. A. R. Howlider, A. Iwasawa, N. Yoshizaki, The magnum-isthmus junction of the fowl oviduct participates in the formation of the avian-type shell membrane. *Zool. Sci.* **23**, 41–47 (2006).

20. A. Mallock, The shapes of birds' eggs. *Nature*. **116**, 311–312 (1925).

21. D. W. Thompson, *On growth and form.* (Cambridge Univ. Press, 1942).

22. J. Okabe, On the forms of hen's eggs. *Reports of Research Institute for Applied Mechanics*. **1**, 7–30 (1952).

23. E. A. Evans, R. Skalak, Mechanics and Thermodynamics of Biomembranes. *Boca Raton, FL: CRC Press* (1980).

24. A. Goriely, M. Tabor, Biomechanical models of hyphal growth in actinomycetes. *J. Theor. Biol.* **222**, 211–218 (2003).

25. D. A. Balch, C. Tyler, Variation in some shell membrane characteristics over different parts of the same shell. *Bri. Poult. Sci.* **5**, 201–215 (1964).

26. R. O. Prum *et al.*, A comprehensive phylogeny of birds (Aves) using targeted next-generation DNA sequencing. *Nature* (2015), doi:10.1038/nature15697.

27. W. Jetz, D. B. Thomas, J. B. Joy, K. Hartmann, A. O. Mooers, The global diversity of birds in space and time. *Nature*. **491**, 444–448 (2012).

28. R. Lockwood, J. P. Swaddle, J. Rayner, Avian wingtip shape reconsidered: wingtip shape indices and morphological adaptations to migration. *J. Avian Biol.* (1998).

29. S. Claramunt, E. P. Derryberry, J. V. Remsen, R. T. Brumfield, High dispersal ability inhibits speciation in a continental radiation of passerine birds. *Proc. R. Soc. London Ser. B.* **279**, 1567–1574 (2012).

30. X. Zheng *et al.*, Preservation of ovarian follicles reveals early evolution of avian reproductive behaviour. *Nature*. **495**, 507–511 (2013).

31. G. Grellet-Tinner, L. Chiappe, M. Norell, D. Bottjer, Dinosaur eggs and nesting behaviors: A paleobiological investigation. *Palaeogeogr. Palaeoclimatol. Palaeoecol.* **232**, 294–321 (2006).

32. T. Sato, A Pair of Shelled Eggs Inside A Female Dinosaur. *Science*. **308**, 375–375 (2005).

33. M. Walters, *Birds' eggs* (DK Publishing, New York, 1994).

34. F. W. Preston, The shapes of birds' eggs: mathematical aspects. *Auk*, 454–463 (1968).

35. H. S. M. Coxeter, *Introduction to Geometry* (Wiley New York, 1969), vol. 136.

36. L. Edwards, *Projective Geometry* (Floris Books, Edinburgh, 2003).

37. H. Liang, L. Mahadevan, The shape of a long leaf. *Proc. Natl. Acad. Sci. U.S.A.* **106**, 22049–22054 (2009).

38. T. Savin *et al.*, On the growth and form of the gut. *Nature*. **476**, 57–62 (2011).

39. J. Zhou *et al.*, Elaborate architecture of the hierarchical hen's eggshell. *Nano. Res.* **4**, 171–179 (2010).

40. A. Lazarus, H. C. B. Florijn, P. M. Reis, Geometry-Induced Rigidity in Nonspherical Pressurized Elastic Shells. *Phys. Rev. Lett.* **109**, 144301 (2012).

41. D. Vella, A. Ajdari, A. Vaziri, A. Boudaoud, Indentation of Ellipsoidal and Cylindrical Elastic Shells. *Phys. Rev. Lett.* **109**, 144302 (2012).

42. W. Jetz, C. H. Sekercioglu, K. Böhning-Gaese, The worldwide variation in avian clutch size across species and space. *Plos. Biol.* **6**, e303 (2008).

43. J. del Hoyo, A. Elliott, J. Sargatal, D. A. Christie, E. de Juana, Handbook of the Birds of the World Alive. Lynx Edicions, Barcelona (2014).

44. H. Wilman *et al.*, EltonTraits 1.0: Species-level foraging attributes of the world's birds and mammals: Ecological Archives E095-178. *Ecology*. **95**, 2027–2027 (2014).

45. A. L. Pigot, J. A. Tobias, Dispersal and the transition to sympatry in vertebrates. *Proc. R. Soc. London Ser. B.* (2015), doi:10.1126/science.1215182.

46. A. L. Pigot, C. H. Trisos, J. A. Tobias, Functional traits reveal the expansion and packing of ecological niche space underlying an elevational diversity gradient in passerine birds. *Proc. R. Soc. London Ser. B.* **283**, 20152013 (2016).

47. B. A. Dawideit, A. B. Phillimore, I. Laube, B. Leisler, K. Böhning-Gaese, Ecomorphological predictors of natal dispersal distances in birds. *J Anim Ecology*. **78**, 388–395 (2009).

48. Hosner *et al.*, How do seemingly non-vagile clades accomplish trans-marine dispersal? Trait and dispersal evolution in the landfowl (Aves: Galliformes) *In Press*.

49. J. D. Kennedy *et al.*, The influence of wing morphology upon the dispersal, geographical distributions and diversification of the Corvides (Aves; Passeriformes). *Proc. R. Soc. London Ser. B.* **283**, 20161922 (2016).

50. J. M. Rayner, Form and function in avian flight, 1–66 (1988).

51. U. M. Norberg, J. Rayner, Ecological morphology and flight in bats (Mammalia; Chiroptera): wing adaptations, flight performance, foraging strategy and echolocation. *Proc. R. Soc. London Ser. B.* (1987).

52. J. D. Kennedy *et al.*, Ecological limits on diversification of the Himalayan core Corvoidea. *Evolution*. **66**, 2599–2613 (2012).

53. L. Jenni, R. Winkler, The feather-length of small passerines: a measurement for wing-length in live birds and museum skins. *Bird Study* (1989), doi:10.1139/z79-308.

54. J. M. Starck, in *Current Ornithology* (Springer, 1993), pp. 275–366.

55. J. B. Dunning Jr, *CRC Handbook of Avian Body Masses, Second Edition* (CRC Press, ed. 2, 2007).

56. R. J. Hijmans, S. E. Cameron, J. L. Parra, P. G. Jones, A. Jarvis, Very high resolution interpolated climate surfaces for global land areas. *Int. J. Climatol.* **25**, 1965–1978 (2005).

57. L. J. Revell, phytools: an R package for phylogenetic comparative biology (and other things). *Methods Ecol Evol*. **3**, 217–223 (2011).

58. J. D. Hadfield, MCMC methods for multi-response generalized linear mixed models: the MCMCglmm R package. *J. Stat. Softw.* (2010).

59. M. N. Puttick, G. H. Thomas, M. J. Benton, High rates of evolution preceded the origin of birds. *Evolution*. **68**, 1497–1510 (2014).

60. P. F. Battley *et al.*, Empirical evidence for differential organ reductions during trans-oceanic bird flight. *Proc. R. Soc. London Ser. B.* **267**, 191–195 (2000).

61. S. Chatterjee, *The Rise of Birds: 225 Million Years of Evolution* (JHU Press, 2015).

62. X. Wang *et al.*, Eggshell and Histology Provide Insight on the Life History of a Pterosaur with Two Functional Ovaries. *An. Acad. Bras. Cienc.* **87**, 1599–1609 (2015).

63. A. Salamon, J. P. Kent, Orientation of the Egg at Laying-Is the Pointed or the Blunt End First? *Int. J. Poult. Sci.* (2014).